University of Kent

Kent Academic Repository

Elzein, Ahmed, Sideris, Nikolaos, Dixon, Alexander C., Galvácsi, Antal, Bodnár, Nikolett, Kállay, Csilla, Lesiów, Monika Katarzyna, Devonport, Jack, Essien, Nsikak B., Wai, Su and others (2026) ***Salpyran ligands at the interface of copper chemistry and biology: structure–function relationships, metal selectivity, redox control, and biological interactions.*** **Dalton Transactions . ISSN 1477-9226.**

Downloaded from

https://kar.kent.ac.uk/117851/ The University of Kent's Academic Repository KAR

The version of record is available from

https://doi.org/10.1039/d6dt02297a

This document version

Publisher pdf

DOI for this version

Licence for this version

CC BY-NC (Attribution-NonCommercial)

Additional information

Versions of research works

Versions of Record

If this version is the version of record, it is the same as the published version available on the publisher's web site. Cite as the published version.

Author Accepted Manuscripts

If this document is identified as the Author Accepted Manuscript it is the version after peer review but before type setting, copy editing or publisher branding. Cite as Surname, Initial. (Year) 'Title of article'. To be published in ***Title of Journal*** , Volume and issue numbers [peer-reviewed accepted version]. Available at: DOI or URL (Accessed: date).

Enquiries

If you have questions about this document contact ResearchSupport@kent.ac.uk. Please include the URL of the record in KAR. If you believe that your, or a third party's rights have been compromised through this document please see our Take Down policy (available from https://www.kent.ac.uk/guides/kar-the-kent-academic-repository#policies).

Dalton Transactions

ROYAL SOCIETY OF CHEMISTRY

PAPER

Published on 04 November 2026
Licensed under CC-BY-NC 4.0

Check for updates

Cite this: DOI: 10.1039/d6dt02297a

Salpyran ligands at the interface of copper chemistry and biology: structure–function relationships, metal selectivity, redox control, and biological interactions

Ahmed Elzein,[a] Nikolaos Sideris,[b] Alexander C. Dixon,[a] Antal Galvácsi,[c] Nikolett Bodnár,[c] Csilla Kállay, *[c] Monika Katarzyna Lesiów, *[d] Jack Devonport,[a] Nsikak B. Essien,[a] Su Wai,[a] Rupert Purchase, [a] George Firth, [e] John Spencer, [a,f] Petra Lippmann,[g] Ingo Ott, [g] Martin Michaelis,[h,i] Mark Wass,[h] Jindrich Cinatl,[h,i] Jessica Booth,[f] Kay Osborn,[f] Erika J. Mancini,[b,f] Leandro Castellano[b] and George E. Kostakis *†[a]

This study evaluates Salpyran, a tetradentate N_3O ligand, and electronically modified derivatives. Systematic potentiometry reveals that substituent effects modestly modulate metal binding without significantly improving Cu(II)/Zn(II) selectivity. Direct comparison with trientine identifies an unexpected Fe(III) preference for Salpyran, thus limiting its application as a copper-selective chelator but provides key design principles for future structural refinement. Our data shows that. Cu(II)–Salpyran suppresses ROS generation, protects peptides from oxidation, and binds DNA non-oxidatively. Proof-of-concept ^{64}Cu radiolabelling shows PET imaging compatibility, though Fe(III) competition requires framework refinement. Cytotoxicity studies reveal context-dependent antiproliferative activity: copper coordination enhances potency in most cancer lines but reduces it in carboplatin-resistant NSCLC models, without cross-resistance. This work establishes Salpyran as a versatile platform and provides design principles linking ligand structure, metal selectivity, redox behaviour, and biological activity.

Received 21st September 2026,
Accepted 3rd November 2026

DOI: 10.1039/d6dt02297a

rsc.li/dalton

Introduction

Copper is an essential transition metal involved in numerous biological processes and due to its ability to access multiple oxidation states under physiological conditions plays a central role in redox biology, thus has attracted considerable interest in medicinal chemistry.[1–5] In a number of influential reviews (*e.g.* ref. 6), Sorenson highlighted the potential therapeutic properties of low-molecular-weight copper complexes including their anti-inflammatory, antimicrobial, anticonvulsant, analgesic, and anticancer activities.[6] Since then, extensive efforts have been devoted to understanding how copper coordination influences biological function and to developing copper-based therapeutic agents. Despite considerable progress, establishing predictive relationships between ligand structure, copper speciation, redox behaviour, and biological activity remains a major challenge in bioinorganic chemistry.[7–19]

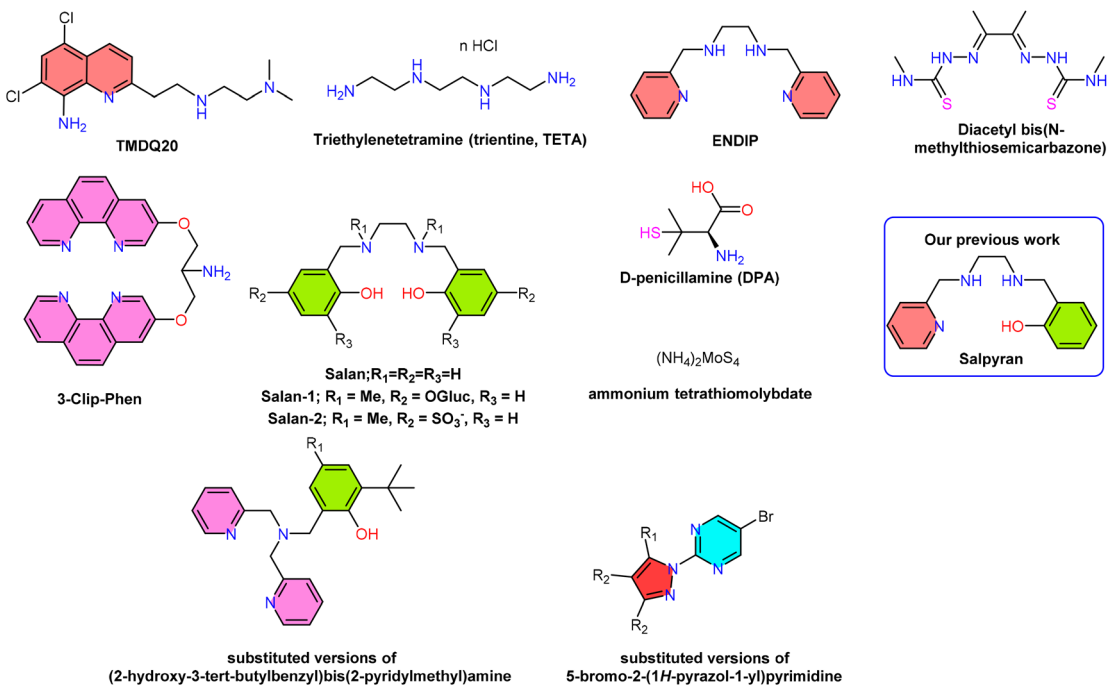
Among the therapeutic applications of copper complexes, their potential use as anticancer agents has received particular attention. In contrast to platinum-based drugs,[20,21] which primarily target DNA, copper compounds frequently exhibit multimodal mechanisms of action involving disruption of metal homeostasis, modulation of cellular signalling pathways, proteotoxic stress, redox imbalance, and oxidative damage. Many biologically active copper systems undergo Cu(I)/Cu(II) redox cycling, generating reactive oxygen species (ROS) such as superoxide and hydroxyl radicals capable of

[a]Department of Chemistry, School of Life Sciences, University of Sussex, Brighton, BN1 9QJ, UK. E-mail: G.Kostakis@sussex.ac.uk
[b]Department of Biochemistry and Biomedicine, School of Life Sciences, University of Sussex, Brighton, BN1 9QG, UK
[c]Department of Inorganic and Analytical Chemistry, University of Debrecen, H-4032 Debrecen, Hungary. E-mail: kallay.csilla@science.unideb.hu
[d]Faculty of Chemistry, University of Wrocław, F. Joliot-Curie 14, 50-383 Wrocław, Poland. E-mail: monika.lesiow2@uwr.edu.pl
[e]School of Biomedical Engineering and Imaging Sciences, King's College London, London, SE1 7EH, UK
[f]Sussex Drug Discovery Centre, School of Life Sciences, University of Sussex, Brighton, BN1 9QJ, UK
[g]Institut für Medizinische und Pharmazeutische Chemie, Technische Universität Braunschweig, Beethovenstr. 55, D-38106 Braunschweig, Germany
[h]School of Natural Sciences, University of Kent, Canterbury, UK
[i]Dr Petra Joh Research Institute, Frankfurt am Main, Germany
† Present address: FZU – Institute of Physics of the Czech Academy of Sciences, Na Slovance 1999/2, Prague 8, 182 00, Czech Republic. E-mail: Kostakis@fzu.cz

inducing cellular damage and apoptosis.[22–24] Consequently, the biological activity of copper complexes is often closely linked to the coordination environment imposed by the ligand. However, predicting how ligand architecture influences copper-mediated oxidative chemistry and downstream biological outcomes remains difficult, limiting the rational design of new copper-based therapeutics.[25–32] Recent medicinal-inorganic studies have converged on copper complexes that kill cancer cells through pro-oxidant mechanisms. For example, Chen and co-workers reported pyrazolopyrimidine Cu(II) complexes that deplete glutathione and generate hydroxyl radicals by Fenton-like chemistry, triggering combined apoptosis and ferroptosis in bladder cancer models.[33] Xu *et al.* described a mitochondria-targeting Cu(I)–triphenylphosphine complex that combines Fenton-like ROS generation with hallmarks of cuproptosis (FDX1 downregulation, lipoylated-DLAT oligomerization, Fe–S cluster loss).[34] Karges and co-workers extended this concept to molecular tripodal N_3O–Cu(II) complexes, which accumulate in mitochondria and induce cuproptosis with nanomolar potency.[35] In each case, biological activity is rationalised through the ability of the copper centre to cycle between oxidation states and to participate in redox chemistry. Whether Cu-based cytotoxicity can be achieved while suppressing this redox chemistry, and what ligand properties would be required to do so, remains unexplored, and motivates the present investigation of the Salpyran platform.

The design of biologically relevant copper ligands therefore requires careful consideration of donor atom composition, coordination geometry, redox accessibility, aqueous stability, and bioavailability. Some copper chelators with potential or proven clinical application are shown in Scheme 1.[36–44] Three of these ligands, trientine, D-penicillamine and tetrathiomolybdate, are used clinically to treat Wilson's disease.[45] The high affinity of trientine for Cu(II) coupled[46–48] with its reduced adverse effect profile compared with that of D-penicillamine are of particular advantage for treating this copper-related storage disorder.[49,50] Nevertheless, polyamine-based ligands are conformationally flexible and often permit multiple coordination geometries in solution. Coordination of these ligands with metal ions can result in dynamic metal speciation and potentially altered redox behaviour.[51,52] These observations highlight the importance of ligand architectures capable of imposing greater structural definition around the metal centre while maintaining favourable physicochemical properties required for biological applications.

As part of our efforts to develop structurally defined copper-binding ligands, we previously introduced Salpyran, a tetradentate N_3O donor ligand derived from pyridine and salicylaldehyde building blocks.[53] Salpyran incorporates three nitrogen donors and one phenolate oxygen donor arranged to form two five-membered and one six-membered chelate rings, providing a rigid coordination framework for Cu(II) binding. The ligand was originally designed as a potential Cu(II)-selective chelator and combines hydrophilic and hydrophobic structural features that enable detailed investigations in aqueous media while maintaining sufficient lipophilicity for biological applications. Initial studies demonstrated strong copper binding and revealed pronounced solvent-dependent effects on complex stability and speciation, highlighting the importance of the surrounding environment in determining metal-ion behaviour.[54–57] Subsequent investigations revealed several unusual features of the Cu-Salpyran system. In contrast to



Scheme 1 Some copper chelating agents with potential or proven clinical application.

This journal is © The Royal Society of Chemistry 2026

many biologically active copper complexes, Cu-Salpyran suppresses ascorbate consumption and inhibits ROS generation under both aerobic and anaerobic conditions. The complex exhibits remarkable resistance towards oxidative degradation, remains stable in the presence of hydrogen peroxide, and limits oxidative modification of peptide and protein fragments in Cu(II)/H_2O_2 assays. Furthermore, Cu-Salpyran inhibits dityrosine cross-link formation in tau protein fragments, a marker of copper-driven oxidative modification. Together, these findings suggest that Salpyran stabilises Cu(II) and suppresses copper-mediated redox chemistry under the conditions examined, distinguishing it from many previously reported copper systems.[36–44,49–52] These observations are chemical in nature and do not establish a general antioxidant effect in cells.

Although Schiff-base, salen-type, and related copper complexes have been extensively investigated as anticancer agents,[2–4,58,59] the biological potential of pyridine-containing salicylaldehyde-derived ligands remains comparatively unexplored. Salpyran represents a particularly attractive scaffold because it combines strong metal-binding ability with tuneable electronic properties, a well-defined coordination environment, and the ability to stabilise Cu(II) under physiologically relevant conditions. However, the consequences of these properties for biological function remain unclear. In particular, the relationship between ligand structure, metal selectivity, copper redox chemistry, DNA interactions, and cellular activity has not previously been examined within the Salpyran framework. To the best of our knowledge, neither Salpyran nor its Cu(II) complexes have been evaluated in cancer cell lines, and no systematic study has explored how structural modification of this ligand family influences both metal-binding and biological properties. Based on this evidence, the objectives of this study were fourfold: (i) to prepare and evaluate a series of Salpyran derivatives in order to establish structure–function relationships governing metal selectivity and complex stability; (ii) to obtain structural and spectroscopic insight into the parent Cu-Salpyran system through EPR and radiolabelling studies; (iii) to investigate the influence of copper coordination on redox behaviour, ROS generation, and interactions with biologically relevant targets, including DNA; using the parent system as the most comprehensively characterized representative of the series; and (iv) to evaluate the *in vitro* cellular activity of Salpyran and Cu-Salpyran in platinum-sensitive and platinum-resistant NSCLC models. Importantly, the derivatisation study serves to define the scope of the current ligand family, with subsequent mechanistic investigations rationally focused on the parent scaffold in the absence of a superior derivative.

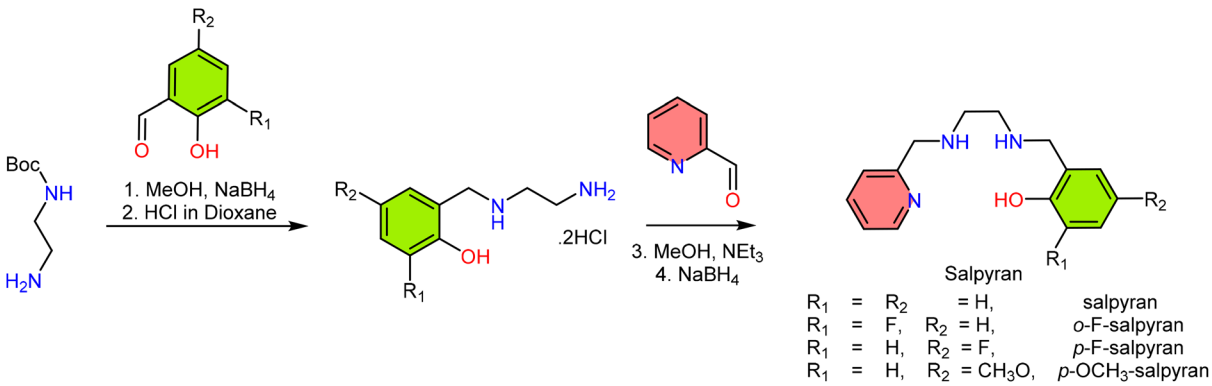
Results

Ligand design and synthesis

Derivatives of Salpyran incorporating methoxy or fluorine groups at various positions on the aromatic ring were synthesised and studied to modulate the metal-binding selectivity of the ligand. The methoxy group, an electron-donating group, was positioned at the *para* location to potentially enhance electron density and the introduction of fluorine at *ortho* or *para* positions was intended to withdraw electron density from the ring *via* its inductive effect but also bearing in mind its impact on medicinal chemistry.[60–63] These structural modifications were designed to probe how electronic effects influence the metal-binding properties of Salpyran, with the aim of establishing whether enhanced selectivity or affinity for specific metal ions could be achieved through targeted functionalisation. The ligands were synthesised in two steps (Scheme 2), modifying our protocol,[53] using distinct types of substituted phenols.

Solution behaviour of Salpyran derivatives

The Salpyran derivatives were investigated to evaluate how electronic modification of the ligand framework influences metal binding and selectivity. Protonation constants, stability constants, and pM values of these derivatives are summarised in Table S1 (SI). Potentiometric measurements showed that Salpyran and all derivatives exhibit four deprotonation steps (Table S1). The lowest p*K* value is assigned to the pyridyl nitrogen, while the highest corresponds to deprotonation of the phenolic hydroxyl group; the intermediate values arise from



Scheme 2 Synthetic route towards Salpyran derivatives.

the secondary ammonium functions. Introduction of the electron-donating methoxy group resulted in a systematic increase in all deprotonation constants, consistent with resonance stabilisation of negative charge. In contrast, the electron-withdrawing *ortho*-fluoro substituent decreased all p*K* values relative to Salpyran, while the *para*-fluoro group produced a weaker effect, except for the pyridyl site, where a slight p*K* increase was observed, reflecting reduced inductive influence at the *para* position. These electronic effects translated into modest variations in complex stability (Table S1), which are more clearly captured by the pM values calculated at pH 7.4 (Fig. 1). Methoxy substitution slightly enhanced complex stability, whereas fluoro substitution led to similar pM values. Importantly, these trends were comparable for both Cu(II) and Zn(II), resulting in similar Cu/Zn pM differences across the ligand series. Within the series examined, none of the derivatives afforded a meaningful improvement in Cu(II)/Zn(II) selectivity relative to the parent scaffold, and the parent Salpyran system therefore represents the most suitable point of departure for the subsequent mechanistic and biological investigations reported here. We note that this conclusion is restricted to the electronically accessible, water-soluble derivatives studied; a wider Hammett series, including strongly electron-donating or electron-withdrawing substituents, would be required to establish a general structure-selectivity trend, and is identified as future work.

Solution behaviour of Salpyran *versus* trientine

As the introduction of methoxy and fluoro substituents on the Salpyran scaffold did not lead to a meaningful improvement in Cu(II)/Zn(II) selectivity (Table S1), we extended our investigation to a direct comparison between Salpyran and trientine (Table S2). This comparison was undertaken to evaluate whether Salpyran could serve as a viable alternative to trientine in bioinorganic applications but also to assess their response to other biological important divalent ions and document preference. Potentiometric data for trientine have been reported previously,[46–48] and the values obtained in this study are fully consistent with those literature reports. For clarity and internal consistency, all measurements were recorded under identical experimental conditions and extended to include additional transition metal ions. Trientine, like Salpyran, possesses four protonation sites, all associated with nitrogen donor atoms. The corresponding protonation constants are listed in Table S3. The two lowest p*K* values are assigned to the secondary amine groups, while the higher values correspond to the terminal primary amines. The small separation between the third and fourth protonation constants, approaching the statistical limit, suggests partially overlapping deprotonation processes rather than discrete, independent steps.

The titration curves and calculated species distribution diagrams for all systems are provided in Fig. S1. For both ligands, the dominant species across a broad pH range is the fully coordinated $[ML]^{+}$ complex, in which all donor atoms participate in metal binding. This species predominates under physiological conditions for Cu(II), Zn(II), Co(II), and Fe(II), while for Mn(II) its formation is shifted to higher pH values. Minor amounts of the protonated $[MLH]^{2+}$ species are also observed for Cu(II), Co(II), and Fe(II), reflecting partial protonation of a terminal amine. In the Zn(II) and Fe(II) systems, formation of the deprotonated $[MLH_{-1}]$ species indicates the presence of mixed ligand-hydroxido species.

To facilitate a clearer comparison of metal-binding efficiencies under biologically relevant conditions, the free metal ion concentrations (pM values) calculated at pH 7.4 are summarised in Fig. 2, while the corresponding stability constants are reported in Table S3. The heatmap representation highlights that Salpyran and trientine display comparable binding strengths toward divalent metal ions, particularly Cu(II), for which both ligands exhibit remarkably high pM values (13.30 and 13.35, respectively). In contrast, both ligands show limited Mn(II) binding at physiological pH. A key distinction emerges for Fe(III). While meaningful pM values could not be obtained for the trientine-Fe(III) system due to precipitation at low pH (~2.2), Salpyran forms stable Fe(III) complexes with a pM of 15.25 at pH 7.4. This corresponds to a higher preference for Fe(III) (ΔpM ≈ 1.95) than for Cu(II) under the same conditions, and clearly distinguishes Salpyran from trientine, whose interaction with Fe(III) under comparable conditions leads to insoluble species.

At pH 7.4 and with both metals present at biologically relevant free concentrations, this difference in pM implies that Fe

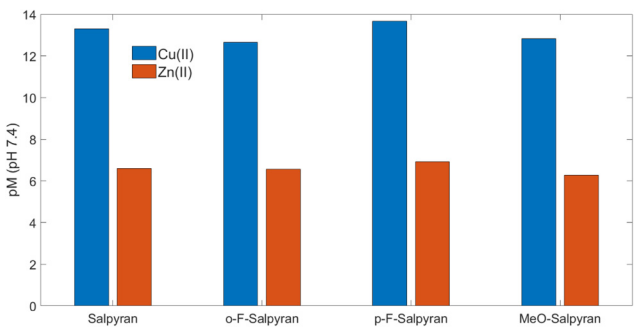


Fig. 1 pM values of Salpyran and its derivatives for Cu(II) and Zn(II) (*I* = 0.2 M KCl, *T* = 25 °C, the pM values were calculated at pH = 7.4 by using 0.01 mM metal ion and ligand concentration).

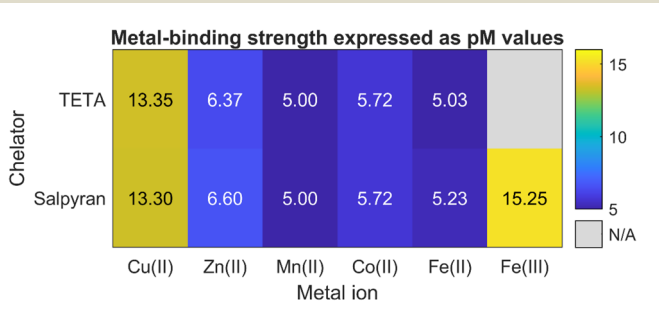


Fig. 2 Heatmap representation of pM values of Salpyran and trientine (TETA) for transition elements (*I* = 0.2 M KCl, *T* = 25 °C, the pM values were calculated at pH = 7.4 by using 0.01 mM metal ion and ligand concentration).

This journal is © The Royal Society of Chemistry 2026

(III) will outcompete Cu(II) for the Salpyran binding site unless the available Fe(III) is strongly buffered (*e.g.* by transferrin). This represents a genuine and previously underappreciated Fe(III) preference within this ligand family and has direct consequences for the proposed Cu-selective applications of the scaffold, as discussed below. Overall, these results demonstrate that Salpyran matches trientine in its Cu(II) binding capability while offering enhanced compatibility with Fe(III), underscoring its potential as a versatile ligand platform for copper bioinorganic chemistry.

Structural characterisation of Cu-Salpyran with EPR at different pH values

The EPR parameters ($A_z(^{63,65}Cu)$ = 18.2 mT, g_z = 2.242, g_y = 2.087, g_x = 2.065) derived from the spectral simulation of the Cu(II)-Salpyran complex at pH 3.0 are indicative of an unsaturated N_3 coordination environment (Fig. 3 and Table 1).[64] These values reflect a complex with axial symmetry, consistent with a tetragonal geometry. Potentiometric studies[53] indicate that at pH 3.0, three species are present: the bis-cationic species $[CuLH]^{2+}$ (83%), the $[CuL]^{+}$ monocationic species (13%), and unbound Cu^{2+} (4%). As the pH increases to 7.4, the $[CuL]^{+}$ species becomes dominant. Given that $[CuLH]^{2+}$ is the most prevalent at pH 3.0, it can be concluded that the N_3O_1 environment is primarily associated with the bis-cationic species in acidic conditions. Upon increasing the pH to 7.4, the A_z value exhibits a modest increase to 19.0 mT, while the g_z value decreases notably to 2.219 (Fig. 3 and Table 1). This variation is likely due to a change in the charge distribution of the complex, which can be attributed to the replacement of the coordinated water molecule in the equatorial coordination plane by the phenoxido oxygen atoms from the ligand. The presence of the phenoxido group alters the electronic environment of the complex and influences the overall charge distribution and coordination geometry, leading to the observed changes in the species present at different pH levels.[64] These studies further validated that the coordination environment depends on the pH, with $[CuLH]^{2+}$ being the key species at lower pH and the

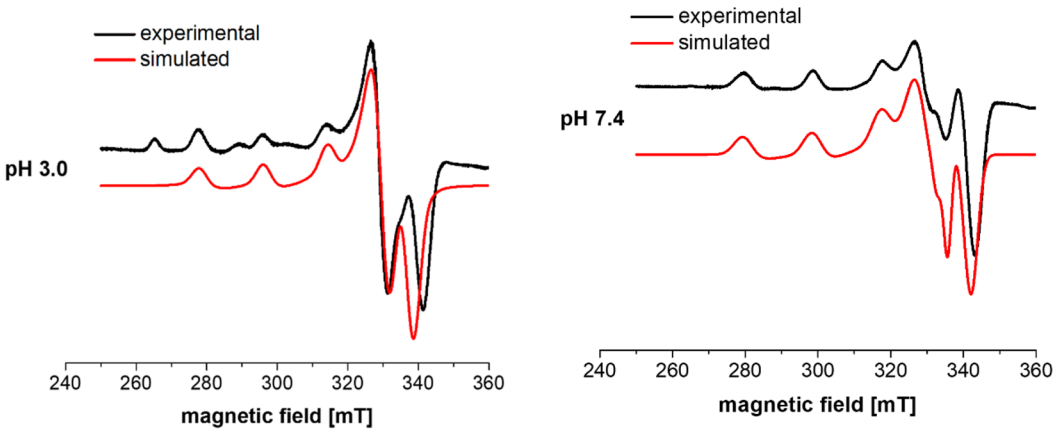
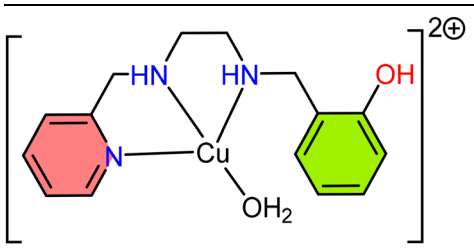
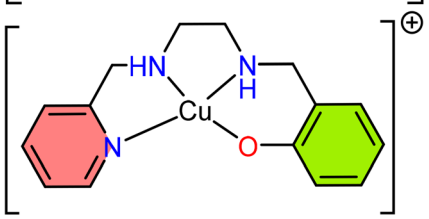


Fig. 3 EPR spectrum recorded for frozen (77 K) solution of Cu(II)-Salpyran complex at pH 3.0 (left) and pH 7.4 (right) (Cu : L = 1 : 1, [Cu(II)] = 0.001 M).

Table 1 EPR parameters of the Cu(II)-Salpyran complex at various pH values (3.0 and 7.4)

pH/structure based on potentiomentry53	EPR parameters	
pH	*g* tensor	Hyperfine coupling [mT]
	g_z = 2.242 g_y = 2.087 g_x = 2.065	$A_z(^{63,65}Cu)$ = 18.2 $A_y(3 \times {}^{14}N)$ = 1.0 $A_x(3 \times {}^{14}N)$ = 1.0
	g_z = 2.219 g_y = 2.085 g_x = 2.045	$A_z(^{63,65}Cu)$ = 19.0

$[CuL]^+$ species being the dominant at physiological pH values. It should be noted that these potentiometric species distributions describe the equilibrium speciation at the respective pH values and do not, by themselves, establish the species responsible for reduction during subsequent reactions with ascorbic acid.

Antioxidant properties with human prion protein HuPrP (103–112)

The effect of the trientine ligand on the oxidation of the human prion protein (HuPrP(103–112), Ac-SKPKTNMKHM-NH_2, abbreviated dMKHM) was investigated. Previous studies have shown that a fragment of the human prion protein undergoes oxidation in the presence of radicals formed from the Cu(II)/H_2O_2 system.[65] The oxidation specifically targets the methionine residues, producing three main products: two singly oxidised products and one doubly oxidised product. The comparison of the amount of the unoxidised peptide in different systems after one hour of oxidation is shown in Fig. 4. After one hour of oxidation, 22% of the HuPrP(103–112) remains intact, while in the presence of Salpyran, almost 60% of the peptide remains unoxidised. Trientine, in comparison, had a lower effect, with 50% of the peptide remaining unoxidised after the same period. In summary, Salpyran proved to be a better alternative to trientine, as it not only offers comparable or slightly higher stability in the formed metal complexes, but also shows greater efficacy in preventing peptide oxidation.

Antioxidant properties with ascorbic acid (EPR and UV-Vis) at different pH values

Previously,[53] we investigated the suppression of copper-mediated oxidation by using two protein fragment oxidation assays and monitoring ascorbic acid consumption by HPLC. These studies demonstrated that the Cu(II)-Salpyran complex suppresses copper-driven oxidation in these assays. Whether this behaviour translates into a functional antioxidant effect in cells or tissues was not established by those experiments and is not claimed here.[66] To further substantiate these findings and to explore alternative approaches for monitoring redox behaviour, we examined the ability of ascorbic acid to reduce Cu(II) to Cu(I) within the Cu(II)-Salpyran complex at pH 3.0 and 7.4 using EPR and UV-Vis spectroscopy. Since the coordination environment of the complex is pH dependent,[53] such changes may directly influence its redox activity and antioxidant capacity.

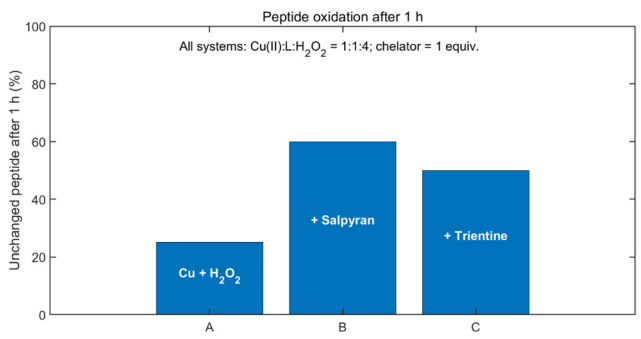


Fig. 4 Amount of unchanged peptide after 1 h oxidation in different Cu(II)/H_2O_2 systems; **A**, Cu(II)–peptide–H_2O_2 (1 : 1 : 4); **B** = **A** + Salpyran (1 equiv.); **C** = **A** + trientine (1 equiv.).

EPR spectra of the Cu(II)-Salpyran complex were first recorded at both pH values, followed by measurements immediately after the addition of ascorbic acid and after 1 h of incubation (Fig. S2). Equimolar concentrations of ascorbic acid and the Cu(II) complex were used throughout (1 : 1 M : L). Reduction of Cu(II) to Cu(I) would result in attenuation or loss of the EPR signal, allowing estimation of the fraction of reduced copper by comparison with the initial spectra. Immediately after the addition of ascorbic acid, no significant reduction of Cu(II) was observed at either pH. After 1 h, however, marked differences emerged. At pH 3.0, approximately 50% of the Cu(II) signal was lost, whereas at pH 7.4 nearly 85% of the copper remained in the +2 oxidation state. These observations demonstrate a pronounced pH dependence in the apparent reduction behavior of the Cu(II)-Salpyran system. A greater degree of Cu(II) reduction under acidic conditions may be linked to pH-dependent changes in the coordination and redox properties of copper complexes. Hydrolysis-related processes may also contribute to these pH-dependent effects, although their precise role remains unclear. In particular, the possibility that reduction of dissociated Cu(II), followed by further dissociation of the coordinated species as the equilibrium is re-established, contributes to the observed signal attenuation cannot be excluded. Although the potentiometric data provide information on the equilibrium distribution of Cu species at each pH, they do not establish the extent to which these species interconvert during the redox experiment. Therefore, the present results do not allow us to distinguish explicitly between reduction of coordinated Cu and reduction following partial complex dissociation. Nevertheless, the substantially lower extent of Cu(II) reduction at pH 7.4 demonstrates that the saturated coordination sphere of copper(II) ions by the 3N,O donor atoms of Salpyran provide protecting role against oxidation and the redox behavior of the system is strongly dependent on pH and its associated coordination environment. On this basis, subsequent experiments were focused on the Cu(II)-Salpyran system at pH 7.4.

To further assess the antioxidant behaviour of the complex under physiological conditions, an ascorbic acid consumption assay was performed at pH 7.4. In systems capable of generating hydroxyl radicals, a rapid decrease in the absorption band of ascorbic acid at 265 nm is typically observed.[67] In the presence of the Cu(II)-Salpyran complex, however, no significant oxidation of ascorbic acid occurred (Fig. 5). The decrease in absorbance at 265 nm was slow and minimal, reaching a plateau after approximately 15 min. Comparison with reported data for other Cu(II) complexes confirms that Cu(II)-Salpyran exhibits pronounced antioxidant behaviour under these conditions.[68–70] The addition of hydrogen peroxide to the reaction mixture with ascorbic acid is expected to accelerate the oxidation of ascorbic acid and enhance hydroxyl radical production in the system.[67] However, the addition of H_2O_2 did not significantly affect the course of

This journal is © The Royal Society of Chemistry 2026

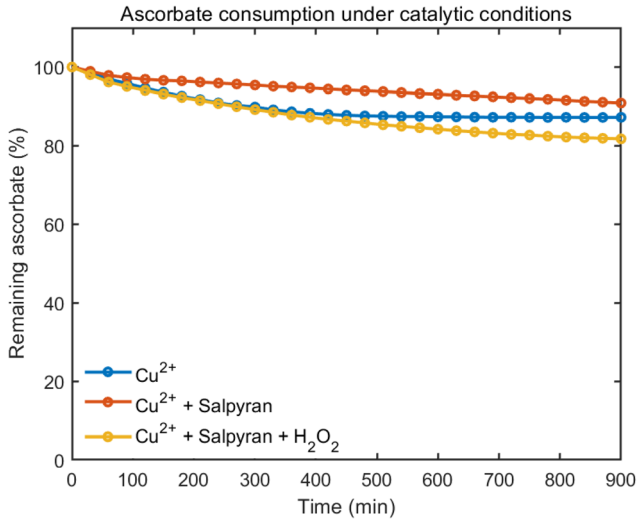


Fig. 5 Ascorbate consumption by Cu(II)-Salpyran with/without H_2O_2 and uncomplexed Cu(II) ions measured by UV spectroscopy (λ = 265 nm) as a function of time.

the reaction, further confirming that Cu(II)-Salpyran is not capable of generating ROS (Fig. 5).

Antioxidant properties. Hydroxyl radical assay

Building on previous experiments demonstrating the limited ability of the Cu(II)-Salpyran complex to oxidise ascorbic acid and generate ROS, we further explored its redox behaviour by directly probing hydroxyl radical formation under comparable conditions. Rhodamine 6G (R6G) was employed as a sensitive hydroxyl radical detector, as its characteristic absorption band at 526 nm decreases upon oxidative degradation.[71]

As shown in Fig. 6, UV-Vis spectra of R6G were recorded at 1 min intervals over 1 h. The control experiment containing R6G alone showed no change in absorbance over time, confirming the stability of the dye under the experimental conditions (Fig. 6, blue trace). In contrast, the addition of uncomplexed Cu(II) ions in the presence of hydrogen peroxide led to a clear and continuous decrease in the absorption band at 526 nm, consistent with efficient hydroxyl radical generation (Fig. 6, red trace).

When the Cu(II)-Salpyran complex was examined under identical conditions, only a minor decrease in absorbance was observed throughout the experiment (Fig. 6, orange trace). This behaviour indicates that complexation by Salpyran strongly suppresses copper-mediated hydroxyl radical formation. The inset bar chart in Fig. 6 further highlights this effect, showing a higher percentage of intact R6G remaining in the Cu(II)-Salpyran system compared to uncomplexed Cu(II).

To further probe the antioxidant capability of Salpyran, the Cu(II)-Prs3 complex-previously reported to exhibit pronounced free radical activity-was investigated in the presence of Salpyran. Prs3 is a peptide fragment derived from presenilin-1, a protein implicated in Alzheimer's disease through oxidative stress pathways.[72,73] Notably, upon addition of Salpyran, degradation of R6G was completely suppressed, with the absorbance trace overlapping closely with that of the R6G control (Fig. 6, purple trace). This observation demonstrates that Salpyran is capable of effectively inhibiting hydroxyl radical formation even in highly reactive copper-peptide systems. Thus concluding, the data presented in Fig. 6 provide direct spectroscopic evidence that Cu(II)-Salpyran does not promote hydroxyl radical generation and instead limits copper-driven oxidative chemistry under the conditions examined. These findings are consistent with reported R6G degradation studies involving known hydroxyl radical-producing systems and further support the antioxidant character of the Cu(II)-Salpyran system.[68,74,75]

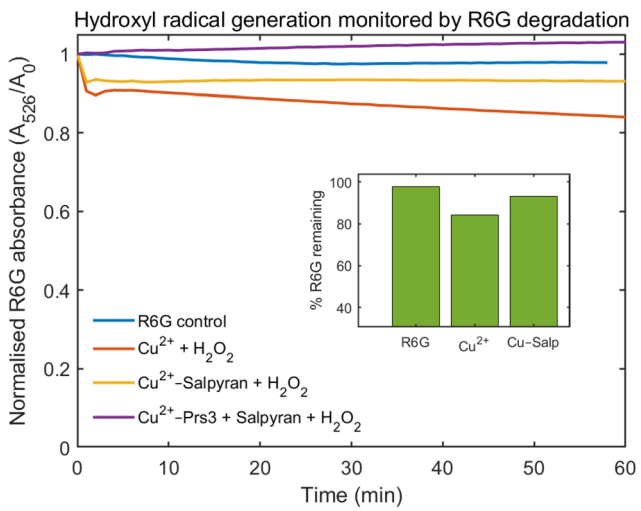


Fig. 6 R6G degradation data. The spectra were measured with 1 minute intervals for 1 hour ([R6G] = 5 μM, Cu : L = 1 : 1.1 molar ratio, [Cu(II)] = 10 μM, [H_2O_2] = 5 mM).

Salpyran radiolabelling with ^{64}Cu

The next step of our study was to explore the potential of the Cu-Salpyran system for visualisation *in vivo*. Positron emission tomography using ^{64}Cu enables non-invasive imaging of copper trafficking and copper-labelled radiopharmaceuticals in animals and humans without the need for invasive biopsies.[76] ^{64}Cu, with its 12.7 hour half-life, is well suited to longitudinal imaging studies over a few days and has been used to study mechanism of trientine and penicillamine chelation therapy in humans.[77] ^{64}Cu has also been used to study copper handling in humans with Wilson's disease and cancer,[78–80] and mouse models of Alzheimer's disease.[81] Salpyran (1 mg) was reacted with $^{64}CuCl_2$ solutions (10 MBq, in 0.1 M ammonium acetate adjusted to pH 5.5, 7, or 8.5) at 50 °C for 30 minutes. Reverse-phase radio-HPLC analysis revealed two major radiolabelled products: one hydrophilic species (~30% radiochemical yield, RCY) and a lipophilic complex (retention times of 8.5 and 21 minutes, respectively; Fig. 7). Both species had different retention times to [^{64}Cu]$CuCl_2$ which eluted at the solvent front (retention time 4.5 min) suggesting complexation. Importantly, the radioactive peak associated with the more lipophilic complex coincided with the UV signal of

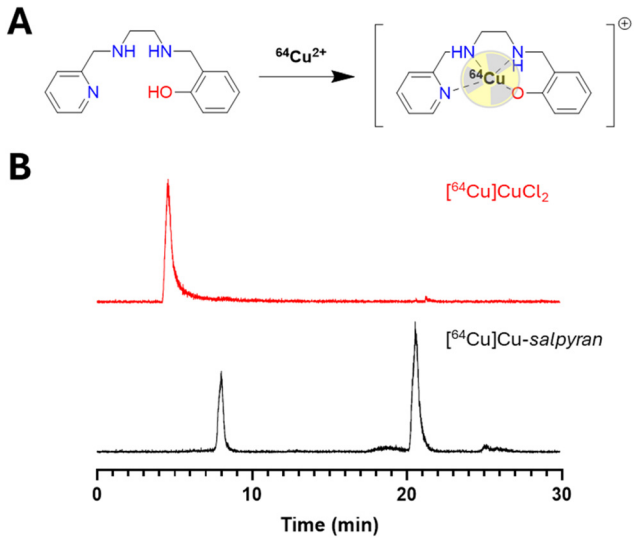


Fig. 7 (A) Radiolabelling scheme for [^{64}Cu]Cu-Salpyran; (B) RP-HPLC radio chromatograms for [^{64}Cu]$CuCl_2$ (top) and [^{64}Cu]Cu-Salpyran reaction after 30 minutes at 50 °C.

the nonradioactive ^{nat}Cu-Salpyran complex. To achieve quantitative radiolabelling of a single radioactive species, ligand quantities and reaction buffers will be needed to be optimised. Alternatively, [^{64}Cu]Cu-Salpyran can be isolated *via* RP-HPLC, purified using C18 Sep-pak, eluted with ethanol, dried, and reconstituted in saline for biological studies. The present results demonstrate that the Salpyran framework is chemically compatible with ^{64}Cu incorporation, establishing proof-of-concept for potential radiochemical applications. However, in light of the new potentiometric data presented in this work, revealing that Salpyran exhibits a pronounced preference for Fe(III) over Cu(II) (ΔpM ≈ 1.95 at pH 7.4; Fig. 2 and Table S3), quantitative radiolabelling would require structural modifications to suppress Fe(III) affinity. In practice, this means that any Salpyran-derived chelator intended for ^{64}Cu PET must either (i) be used under conditions where Fe(III) is effectively buffered (*e.g.* in the presence of excess transferrin or citrate), or (ii) be structurally modified to reduce Fe(III) affinity without compromising Cu(II) affinity. The latter is the more robust long-term solution and is discussed in the following section. Rather than pursuing further optimisation of the current scaffold, we consider these findings as valuable guidance for the future design of Salpyran-inspired frameworks with improved metal selectivity for radiochemical applications.

Interaction of Salpyran and its Cu(II) complex with biological-related molecules

In recent years, the search for new potential cancer drugs has intensified due to alarming cancer incidence statistics. It is estimated that from 2020 to 2040, cancer cases will increase by approximately 50%.[82] Understanding the mechanism of action of potential drugs is critical in designing new chemotherapies.[83] One important aspect of drug development is the interaction of potential drugs with biomolecules, especially DNA. In this context, we examined two distinct questions: (i) whether Salpyran and Cu-Salpyran cause DNA strand breakage, using a plasmid-based assay, and (ii) whether the Cu(II) complex associates with DNA non-covalently, using UV-Vis and CD spectroscopy. These experiments address distinct aspects of DNA interaction, chemical damage *versus* binding mode, and are interpreted separately below. We evaluated different concentrations of Salpyran (250 μM, 100 μM, 50 μM, 20 μM, and 10 μM) and its Cu(II) complex (at the same concentrations) against plasmid DNA. The native plasmid DNA (form I), known as supercoiled form, migrates the fastest during agarose gel electrophoresis due to its compact conformation. A single-strand break converts the supercoiled DNA into the open circular (form II) conformation, which migrates the slowest because of its relaxed structure. Double-strand breaks generate the linear DNA (form III), which migrates at an intermediate rate between the supercoiled and open circular forms. The electropherogram shows that Salpyran alone (regardless of concentration) causes DNA strand damage and the formation of a circular DNA form (Fig. 8A and B, lanes 3, 6, 9, 12, 15, with approximately 30% of form II in each case). In contrast, the Cu(II)-Salpyran complex at concentrations of 250–50 μM is more aggressive towards DNA (Fig. 8A and B, lanes 4, 7, and 10). It induces double-strand breaks, with about 50% of the DNA in the linear form (form III), and the native form is absent. When the complex concentration is lowered to 20 μM, both circular and linear forms of DNA are observed (Fig. 8A and B, lane 13), with 60% of form II and 10% of form III, while the super helical form (form I) is still present (30%). At the lowest concentration tested (10 μM), no form III DNA is observed, and the native form of DNA predominates (about 70%), with approximately 30% in the circular form (Fig. 8A and B, lane 16).

The plasmid assay therefore demonstrates concentration-dependent DNA strand breakage by Cu(II)-Salpyran (and, to a lesser extent, by the free ligand) under these conditions. Because the redox experiments above show that the complex does not generate hydroxy radical, this cleavage is unlikely to be radical-mediated and may instead reflect a direct, non-oxidative interaction with DNA. Importantly, this experiment reports the consequence of DNA interaction (strand breakage) and does not by itself identify the binding mode. To investigate further, we performed UV-Vis spectroscopy and circular dichroism (CD) experiments using calf thymus DNA (ctDNA). DNA interactions with compounds can be covalent or non-covalent, but covalent interactions are rare for Cu(II) complexes. Non-covalent interactions most commonly include electrostatic interactions, groove binding, and intercalation.[84] Intercalation typically leads to bathochromic and hypochromic effects,[85,86] while hyperchromism is associated with electrostatic interactions or partial DNA helix unwinding.[87] UV-Vis absorption spectra of ctDNA with the Cu(II)-Salpyran complex, recorded over 24 hours, show a hyperchromic effect (ΔA_{260} nm = 0.108) (Fig. S3). Hyperchromism is commonly associated with electrostatic or partial helix-unwinding interactions, and

This journal is © The Royal Society of Chemistry 2026

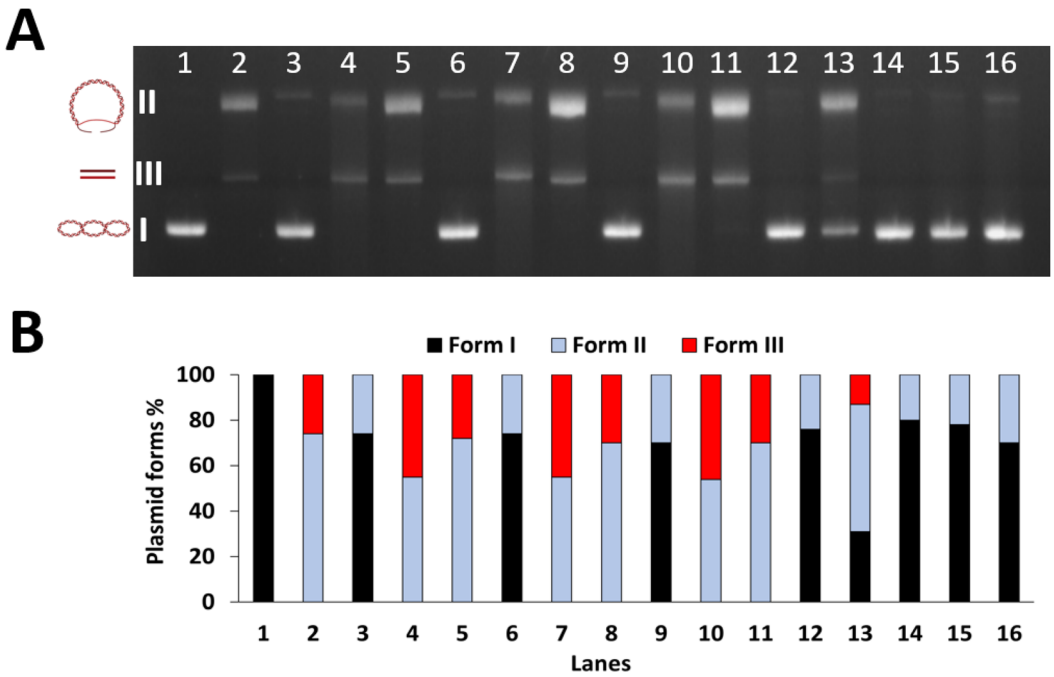


Fig. 8 (A) Agarose gel electrophoresis of pBR322 plasmid (**1**) cleavage and components at different loading: 250 μM; Cu(II) (**2**), Salpyran (**3**), Cu(II)-Salpyran (**4**), 100 μM; Cu(II) (**5**), Salpyran (**6**), Cu(II)-Salpyran (**7**), 50 μM; Cu(II) (**8**), Salpyran (**9**), Cu(II)-Salpyran (**10**), 20 μM; Cu(II) (**11**), Salpyran (**12**), Cu(II)-Salpyran (**13**), 10 μM; Cu(II) (**14**), Salpyran (**15**), Cu(II)-Salpyran (**16**) (all lines contain plasmid) and (B) densitometric analysis of the electropherogram.

is therefore consistent with, but not diagnostic of, a predominantly electrostatic interaction between the complex and the DNA backbone. We note that this experiment reports a spectroscopic change rather than a binding mode directly.[87]

The DNA binding ability was further tested using CD spectroscopy. The DNA CD spectrum shows a negative cotton effect at ~245 nm and a positive one at ~280 nm. The negative band is associated with right-handed helicity, while the positive band corresponds to base pair stacking.[88,89] Electrostatic interactions or groove binding typically cause little to no change in these bands, while intercalation results in an increase in the intensity of both bands.[42] After 1 and 24 hours of incubation with the Cu(II)-Salpyran complex, modifications were observed in both CD bands: an increase in the intensity of the negative band and a decrease in the positive band (Fig. 9). These changes are consistent with Cu(II)-Salpyran inducing conformational changes in DNA (a B- to C-like transition), which would be compatible with electrostatic or groove-associated interactions rather than covalent binding. CD spectroscopy is sensitive to overall DNA conformation and therefore reports the consequence of interaction rather than the binding mode itself; the assignment of a predominantly electrostatic interaction is further supported by the UV-Vis hyperchromism, but a contribution from other non-covalent modes cannot be excluded on the basis of these data alone.

Taken together, the plasmid and spectroscopic experiments should be read as complementary rather than mutually confirmatory. The agarose assay shows that Cu(II)-Salpyran can cause DNA strand breakage at higher concentrations (≥50 μM), whereas the UV-Vis and CD data indicate that the complex associates with DNA non-covalently, through electrostatic interactions. These observations are not in conflict: a non-covalent association can precede and/or accompany strand breakage, and the two experiments probe various stages of the interaction (binding *versus* chemical outcome). The spectroscopic data do not establish the precise binding mode, and the plasmid data do not identify the species responsible for cleavage; together, however, they indicate that Cu(II)-Salpyran interacts with DNA without requiring radical formation, consistent with the redox behaviour described above.

Preliminary cancer cell studies

Establishment and validation of acquired carboplatin resistance models. The derivative series was designed primarily to investigate structure–property relationships governing metal binding, stability, and selectivity. As the electronic modifications resulted in only modest changes in Cu(II)/Zn(II) discrimination and did not improve the overall metal-binding profile relative to the parent scaffold, subsequent biological investigations focused on Salpyran and Cu-Salpyran as representative systems. To validate the acquired resistance phenotype, parental and carboplatin-resistant A549 and HCC827 cells were treated with increasing concentrations of carboplatin and analysed using four-parameter log-logistic (LL.4) dose–response modelling. Resistant cells displayed a rightward shift in dose–response curves compared with parental controls

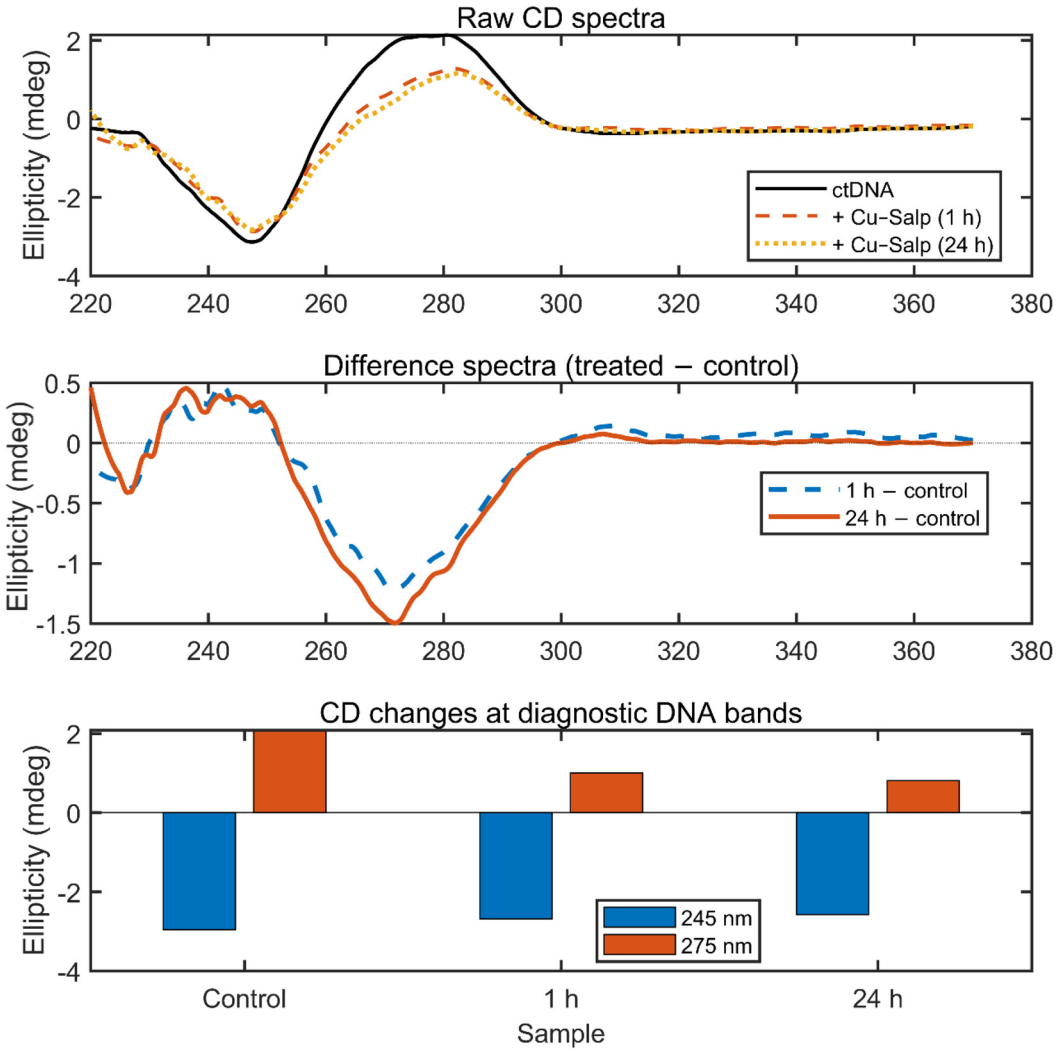


Fig. 9 CD spectra of binding of 10 molar equivalents of the ctDNA with Cu(II)-Salpyran complex (C = 0.22 mM). The samples were prepared in water solution, while the spectra were recorder after 1 and 24 hours.

(Fig. 10), indicating reduced carboplatin sensitivity. This was reflected by significantly increased IC_{50} values in both resistant models. A549 resistant cells showed an IC_{50} increase from 52 μM to 381 μM, corresponding to a 7.3-fold resistance shift (p = 0.007), whereas HCC827 resistant cells increased from 43 μM to 80 μM, representing a 1.9-fold shift (p = 0.004) (Table 2). The greater magnitude of resistance observed in A549 cells indicates cell line-dependent differences in acquired carboplatin resistance.

Comparative cytotoxicity of Salpyran and Cu-Salpyran in NSCLC lines

Following validation of the resistance model, the cytotoxic activity of Salpyran and Cu-Salpyran was evaluated in parental and carboplatin-resistant A549 and HCC827 cells. Representative dose–response curves are shown in Fig. 11, with derived IC_{50} values summarised in Table 3. In parental cell lines, Salpyran and Cu-Salpyran displayed comparable activity, with no statistically significant differences in IC_{50} values observed for A549 parental cells (94.8 μM *vs.* 121.2 μM, p = 0.055) or HCC827 parental cells (174.6 μM *vs.* 124.6 μM, p = 0.367).

In contrast, clear differences were observed in carboplatin-resistant cells. In A549 resistant cells, Salpyran exhibited significantly greater potency than Cu-Salpyran, with IC_{50} values of 74.7 μM and 146.9 μM, respectively (p = 0.004). Similarly, in HCC827 resistant cells, Salpyran displayed an IC_{50} of 92.4 μM compared with 179.2 μM for Cu-Salpyran (p = 0.002). In both resistant models, Cu-Salpyran exhibited approximately two-fold higher IC_{50} values than Salpyran, corresponding to reduced potency following Cu coordination. Although these differences reached statistical significance in the resistant cell lines, the absence of significant differences between parental and resistant cells for either compound suggests that the reduced activity of Cu-Salpyran is more likely related to the intrinsic properties of the Cu complex rather than being solely

 This journal is © The Royal Society of Chemistry 2026

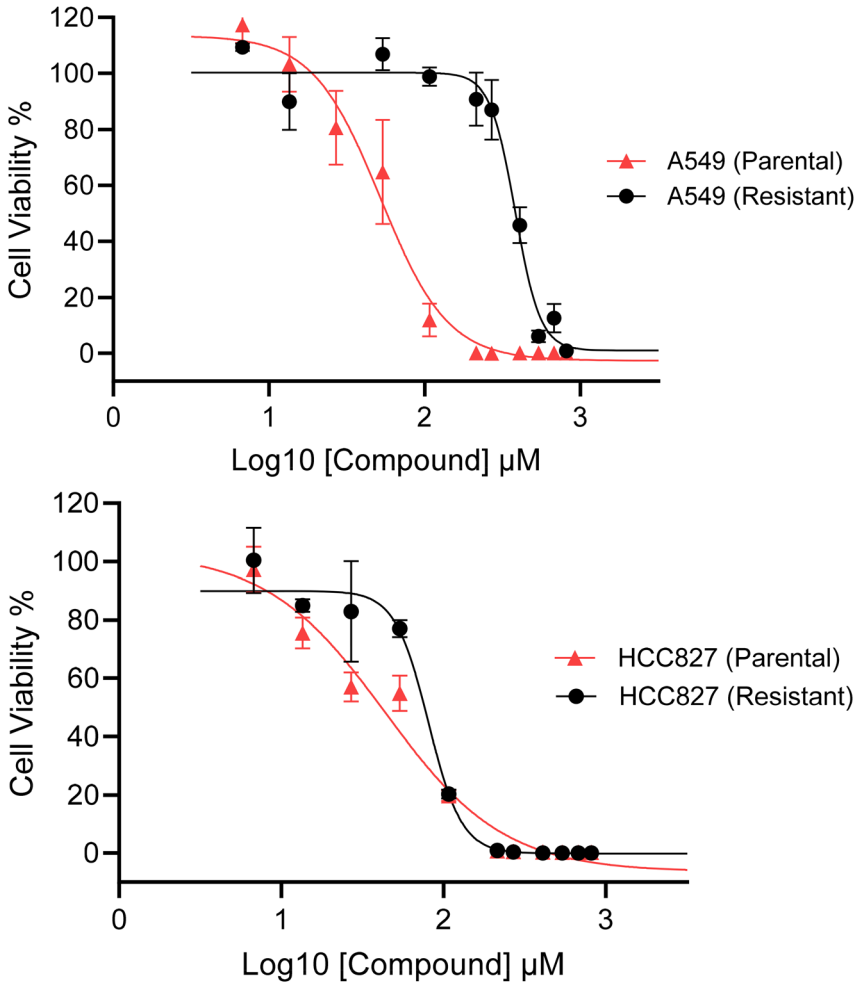


Fig. 10 Carboplatin dose–response curves in parental and resistant A549 and HCC827 cell lines. Cell viability was assessed using the CellTiter-Glo luminescence assay following 72h compound treatment. Dose–response curves were generated and IC_{50} values calculated by nonlinear regression using a four-parameter logistic (4PL) fit. Data are shown as mean ± SEM from $n = 3$ independent biological replicates. Parental (red) and resistant (black) cell lines are shown for A549 (above) and HCC827 (below). Resistance is reflected by a rightward shift in the dose–response curves and corresponding increase in IC_{50} values in resistant cells compared with parental controls.

Table 2 Carboplatin IC_{50} values in parental and resistant A549 and HCC827 cell lines

Cell line	IC_{50} (μM) parental	IC_{50} (μM) resistant	95% CI (parental)	95% CI (resistant)	Fold change (R/P)	*P* Value
A549	52	381	40–64	347–417	7.3	0.007**
HCC827	43	80	18–62	72–90	1.9	0.004**

IC50 values (μM) were calculated by applying nonlinear 4-PL logistic fit to dose response curves. Fold change represents resistance relative to parental controls. Statistical comparisons between parental and resistant cell lines were performed on pIC_{50} values ($n = 3$) using unpaired *t*-tests. $P < 0.01$ is indicated (**). $pIC_{50} = -\log_{10}(IC_{50})$.

driven by the acquired carboplatin-resistance phenotype. These findings were consistent with the leftward shift of Salpyran dose–response curves relative to Cu-Salpyran in resistant cells (Fig. 11), indicating enhanced activity of the metal-free compound under conditions of acquired carboplatin resistance.

Cell viability was assessed using the CellTiter-Glo luminescence assay following 72 h treatment with Salpyran or Cu-Salpyran. Dose–response curves were generated by nonlinear regression using a four-parameter logistic (4PL) model, and IC_{50} values were calculated from the fitted curves. Data are presented as mean ± SEM from $n = 3$ independent biological replicates. Salpyran (red) and Cu-Salpyran (black) dose–response curves are shown for parental A549 (A), resistant A549 (B), parental HCC827 (C), and resistant HCC827 (D) cells. Leftward shifts of the Salpyran dose–response curves relative to Cu-

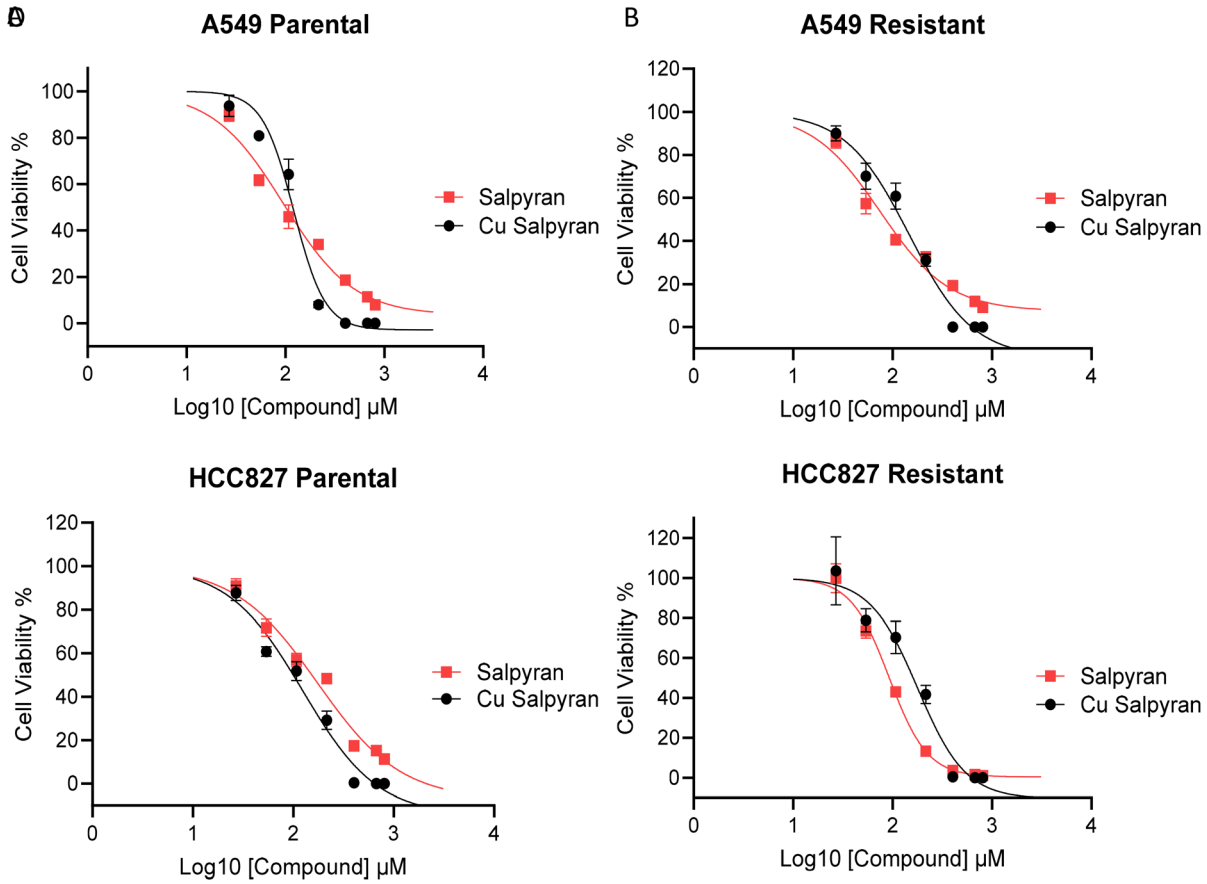


Fig. 11 Comparison of Cu-Salpyran and Salpyran cytotoxicity profile in parental and resistant A549 and HCC827 cell lines.

Table 3 Effect of Salpyran and Cu-Salpyran on cell viability in NSCLC cell lines

Cell line	Salpyran IC50 (μM)	95% CI	Cu–Salpyran IC50 (μM)	95% CI	Fold Change (CS/S)	*p*-Value
A549 parental	94.8	75.8–133.7	121.2	108.8–134.8	1.27	0.055 (ns)
A549 resistant	74.7	60.3–103.9	146.9	117.7–207.4	1.96	0.004 (**)
HCC827 parental	174.6	116.8–454.2	124.6	93.2–209.8	0.71	0.367 (ns)
HCC827 resistant	92.4	85.2–100.5	179.2	140.6–262.0	1.93	0.002 (**)

IC_{50} values (μM) plus 95% confidence intervals (CI) for Salpyran and Cu-Salpyran in parental and carboplatin-resistant cell lines (A549 and HCC827) were obtained by four-parameter logistic (4PL) fit. Statistical comparisons between Salpyran and Cu-Salpyran within each cell line were performed on pIC50 values derived from the corresponding nonlinear regression fits ($n = 3$). Statistical significance was assessed using unpaired *t*-tests and exact *p*-values are shown with significance indicated in brackets (ns, not significant; $^{**}p < 0.01$).

Salpyran indicate greater potency of the metal-free compound, with statistically significant differences observed in both carboplatin-resistant cell lines but not in the corresponding parental cell lines.

To explore whether this differential activity upon Cu coordination extended beyond lung cancer models, preliminary evaluations were conducted across an expanded panel of colorectal cancer cell lines (HT29, RKO, CACO2, COLO205, and COLO320; Fig. S4, S5 and Tables S4, S5). Interestingly, in contrast to the primary NSCLC models, Cu-Salpyran exhibited enhanced potency relative to Salpyran across the majority of colorectal lines tested (*e.g.*, CACO2 IC_{50} = 3.5 μM *vs.* 40.3 μM for Salpyran), suggesting potential lineage-dependent variations in response to copper coordination.

Assessment of cross-resistance to Salpyran and Cu-Salpyran

While carboplatin resistance produced the expected marked reduction in platinum sensitivity (Fig. 10), no comparable shift in sensitivity was observed for either Salpyran or Cu-Salpyran. Direct comparison of parental and carboplatin-resistant cell lines revealed no significant differences in IC_{50} values for either compound, indicating that acquired carboplatin resistance did not confer cross-resistance to Salpyran or Cu-Salpyran under the conditions tested (Fig. 12). Although a stat-

This journal is © The Royal Society of Chemistry 2026

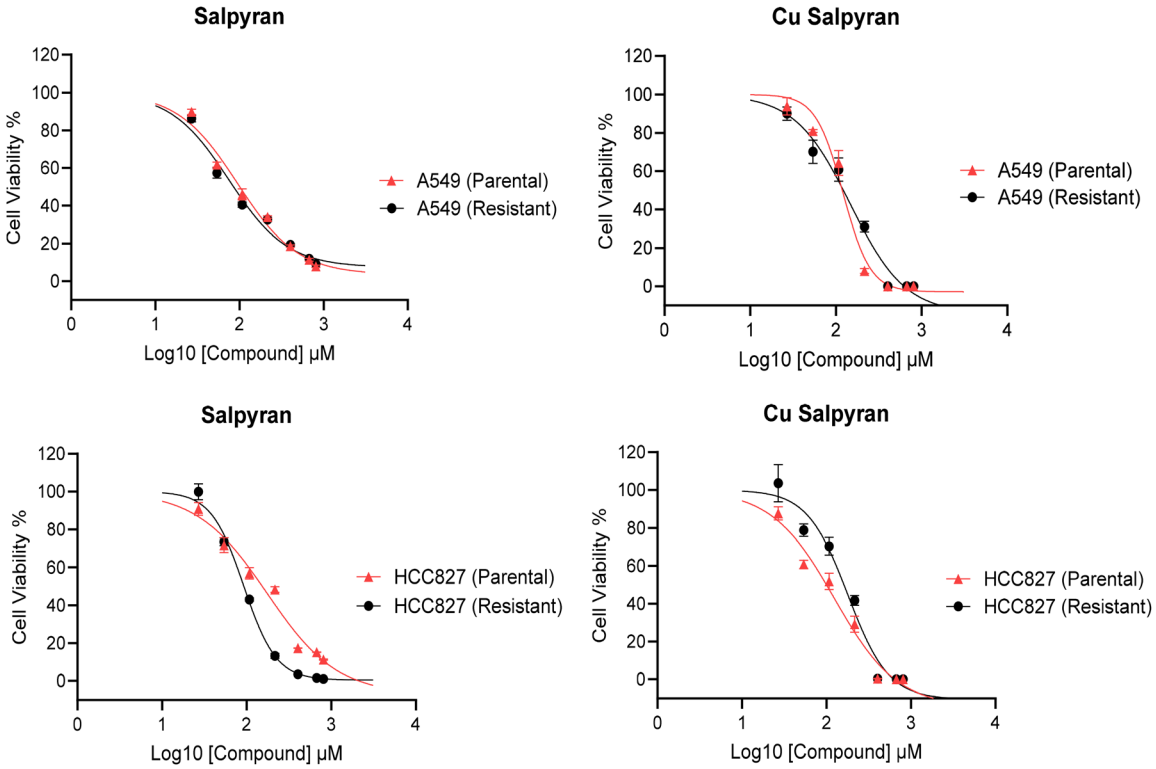


Fig. 12 Comparison of parental and carboplatin-resistant A549 and HCC827 cell line sensitivity to Salpyran and Cu-Salpyran.

istically significant difference was observed in the pIC_{50} comparison for Cu-Salpyran in HCC827 cells, this effect was not supported by separation of the dose–response curve confidence intervals, suggesting limited biological significance (Table 4).

Cell viability was assessed using the CellTiter-Glo luminescence assay following 72 h treatment with Salpyran or Cu-Salpyran. Dose–response curves were generated by nonlinear regression using a four-parameter logistic (4PL) model, and IC_{50} values were calculated from the fitted curves. Data are presented as mean ± SEM from $n = 3$ independent biological replicates. Dose–response curves compare parental and carboplatin-resistant A549 cells treated with Salpyran (A) or Cu-Salpyran (B), and parental and carboplatin-resistant HCC827 cells treated with Salpyran (C) or Cu-Salpyran (D). No substantial shifts in dose–response curves were observed between parental and resistant cells, indicating that acquisition of carboplatin resistance did not confer cross-resistance to either compound under the conditions tested.

Cu-Salpyran produced similar or modestly reduced effects on cell viability compared with Salpyran across both parental and carboplatin-resistant cell lines. Although statistically significant differences between the two compounds were observed in the resistant models, comparison of parental and resistant cells indicated that acquired carboplatin resistance did not significantly alter sensitivity to either compound. These findings suggest that the reduced potency observed following Cu(II) coordination is not associated with a selective

Table 4 Comparison of parental and carboplatin-resistant A549 and HCC827 cell line sensitivity to Salpyran and Cu-Salpyran

Compound	A549 Parental IC_{50} (μM)	95% CI	A549 Resistant IC_{50} (μM)	95% CI	*p*-Value
Salpyran	94.8	75.8–133.7	74.7	60.3–103.9	0.07 (ns)
Cu-Salpyran	121.2	108.8–134.8	146.9	117.7–207.4	0.17 (ns)
Compound	**HCC827 Parental IC_{50} (μM)**	**95% CI**	**HCC827 Resistant IC_{50} (μM)**	**95% CI**	***p*-value**
Salpyran	174.6	116.8–454.2	92.4	85.2–100.5	0.08 (ns)
Cu-Salpyran	124.6	93.2–209.8	179.2	140.6–262.0	0.001 (**)

IC_{50} values (μM) plus 95% confidence intervals (CI) for Salpyran and Cu-Salpyran in parental and carboplatin-resistant A549 and HCC827 cell lines were obtained by four-parameter logistic (4PL) fit. Statistical comparisons between parental and carboplatin-resistant cells were performed separately for Salpyran and Cu-Salpyran using pIC_{50} values derived from the corresponding nonlinear regression fits ($n = 3$). Statistical significance was assessed using unpaired *t*-tests, and exact *p* values are shown with significance indicated in brackets (ns, not significant; $^{**}p < 0.01$).

effect of the carboplatin-resistant phenotype. Overall, Cu(II) coordination did not enhance the ability of Salpyran to reduce cell viability under the conditions tested. Given that both compounds exhibited IC_{50} values in the high micromolar range, the approximately two-fold differences observed between Salpyran and Cu-Salpyran represent modest changes in potency and are unlikely to reflect a substantial improvement in biological activity in these lines. Interestingly, testing across an expanded panel of colorectal cell lines revealed an opposing trend, with Cu-Salpyran displaying enhanced potency over Salpyran in the majority of lines tested (*e.g.*, CACO2, HT29, COLO205; Fig. S4, S5 and Tables S4, S5). Together, these divergent profiles suggest that the biological impact of copper complexation is strongly context-dependent and independent of the carboplatin-resistance phenotype. The altered activity profile following Cu coordination is therefore more likely to reflect changes in physicochemical properties, including cellular uptake, molecular charge distribution, membrane permeability, solution stability, or intracellular speciation, rather than enhanced biological effects such as DNA binding or redox-mediated cytotoxicity. However, the current cellular data do not allow these possibilities to be fully distinguished. As these preliminary findings require further validation, future work is needed to confirm these cell-line trends and investigate compound uptake, intracellular localisation, Cu stability, and target engagement. This will help clarify the mechanism underlying potential tissue selectivity and clarify how metal coordination impacts the cytotoxic properties of these compounds.

Cytotoxicity profiling in additional cancer cell lines

To assess whether the observed activity was restricted to NSCLC models, Salpyran and Cu-Salpyran were further evaluated against a small panel of human cancer cell lines comprising A549 (lung adenocarcinoma), HT-29 (colorectal adenocarcinoma), MCF-7 (breast adenocarcinoma), and MDA-MB-231 (triple-negative breast cancer), together with non-malignant Vero E6 cells. The results are shown in Table 5. For metal-free Salpyran no IC_{50} values could be obtained in the cancer cells up to the highest applied concentration of 50 μM. However, it showed moderate activity against Vero-E6 cells. In contrast, Cu-Salpyran was active against A549, HT-29 cells and Vero-E6 cells, while no IC_{50} could be obtained for this complex in concentrations up to 20 μM in MCF-7 and MDA-MB-231 cells. These findings suggest that Cu binding significantly enhances the intrinsic cytotoxicity of the Salpyran scaffold in several cell types. However, this trend differs from that observed in carboplatin-resistant NSCLC cells, where the free ligand displayed superior activity. Together, the data indicate that the biological response to Salpyran-based systems is highly context dependent and may involve distinct cellular uptake, metal homeostasis, or resistance-associated pathways.

Table 5 Cytotoxicity of salpyran and Cu-Salpyran against several cell lines (IC_{50} values, μM)

	A549	HT-29	MCF-7	MDA-MB-231	Vero-E6
Salpyran	>50	>50	>50	>50	24.8 (±1.2)
Cu-Salpyran	14.5 (±2.4)	12.7 (±0.5)	>20	>20	14.0 (±3.3)

Discussion

Recent theoretical and modelling studies by others have proposed that subtle ligand substituent effects can play a decisive role in modulating copper chelation strength and redox behaviour, particularly in the context of neurodegenerative disease.[90] While these studies provided valuable conceptual frameworks, experimental validation of such predictions has remained limited. Herein, we investigated substituent effects on metal binding and selectivity under fully aqueous conditions, avoiding the use of organic co-solvents that may perturb biomolecular structure.[55–57] Although methoxy- and fluoro-substituted derivatives were successfully prepared and provided valuable insight into the electronic factors governing metal binding, the modifications produced only modest changes in complex stability and did not result in a meaningful improvement in divalent CuZn selectivity relative to the parent scaffold. Consequently, no derivative emerged as a clearly superior candidate for biological evaluation. This outcome, while perhaps unexpected, serves an important purpose: it defines the scope of the current ligand family and provides a clear structure-based rationale for focusing subsequent mechanistic and cellular studies on Salpyran and Cu-Salpyran as the most comprehensively characterised and representative members of the series.

A direct and quantitative comparison with trientine was undertaken across multiple biologically relevant metal ions, which identified that Salpyran exhibits a strong preference for Fe(III) over Cu(II), whereas trientine undergoes Fe(III)-induced precipitation under similar conditions. This observation identifies a key limitation of the parent Salpyran ligand for Wilson's disease therapy while simultaneously providing valuable guidance for future ligand design.

The pronounced Fe(III) affinity of Salpyran (pM = 15.25 at pH 7.4, compared with 13.30 for Cu(II); $\Delta pM \approx 1.95$) is one of the most consequential findings of this work, because it directly constrains the contexts in which the scaffold can be considered Cu-selective. Neither the mitochondria-targeting Cu(I) system[34] nor the tripodal Cu(II) series addresses competition from Zn(II) or Fe(III) under physiological conditions.[35] The present work shows that this is not a peripheral issue, since Salpyran itself has strong preference for Fe(III) over Cu(II). The Fe(III) affinity identified here therefore represents a design constraint that is likely to apply more broadly to N_3O-type copper chelators, and it reinforces the need for explicit metal-selectivity profiling in the development of copper therapeutics.[33–35] Under typical extracellular conditions, Fe(III) is largely bound to transferrin ($\log K \approx 20$), so the free Fe(III) concentration is very low and the competition may be less severe than the pM values alone suggest. Inside cells, however,

 This journal is © The Royal Society of Chemistry 2026

labile iron pools and ferritin turnover can transiently raise free Fe(III), and in Wilson's disease, the main clinical context for copper chelators, hepatic Fe overload is a recognised complication. In both settings, a ligand with such preference for Fe(III) over Cu(II) is unlikely to behave as a Cu-selective chelator and may instead redistribute Fe. This does not invalidate the scaffold, indeed, the redox-suppressing behaviour of Cu-Salpyran remains mechanistically interesting, but it does mean that the Fe(III) affinity must be addressed before Salpyran-derived systems can be proposed for Cu-selective chelation or ^{64}Cu radiochemistry.

Several ligand-design strategies could reduce Fe(III) affinity while preserving Cu(II) binding, provided that aqueous solubility, essential for the potentiometric and biological work reported here, is retained. Fe(III) is a hard, six-coordinate ion that favours O-donors, whereas Cu(II) tolerates softer N-donors and lower coordination numbers; the Salpyran N_3O set is therefore well matched to both metals. Softening one donor (*e.g.* replacing a pyridyl with a thioether or imidazole), enforcing a distorted four-coordinate geometry around Cu(II) *via* steric bulk, or lowering the phenolate pK_a would all be expected to disfavour Fe(III) more than Cu(II), albeit with some cost to Cu(II) affinity and, potentially, to solubility. Any such modification must therefore preserve the hydrophilic/hydrophobic balance of the parent scaffold; the MeO- and F-substituted derivatives examined here probe only a narrow pK_a range (Δp$K_a \approx 0.3$–0.7), consistent with the modest selectivity changes observed, and a wider electronic sweep combined with donor-atom and steric modifications would be the logical next step. These remain design hypotheses rather than demonstrated solutions: the present data establish the Fe(III) problem, but not yet its resolution.

Beyond metal binding, we present new insights into the redox behaviour of the Cu-Salpyran system. Through complementary EPR, UV-Vis, peptide oxidation, and hydroxyl radical detection assays, we demonstrate that Cu-Salpyran does not promote Fenton-type chemistry and can suppress radical generation in highly reactive copper–peptide systems under the conditions examined. The absence of ROS involvement suggests that DNA cleavage may involve non-oxidative pathways, as reported for other Cu(II) complexes under non-oxidative conditions.[91–93] The plasmid and spectroscopic data should nevertheless be kept distinct: the former demonstrate strand breakage, whereas the latter are consistent with non-covalent association. Whether cleavage arises from a DNA-bound Cu-Salpyran species, from a hydrolysis-type mechanism, or from a minor reactive fraction not detected in the bulk assays cannot be resolved from the present data. These experimentally derived observations provide are consistent with mechanistic hypotheses previously inferred from modelling studies, while extending them to peptide-based systems. It should be emphasised that these experiments probe the chemical behaviour of Cu-Salpyran in defined aqueous and peptide-based systems. They establish that the complex suppresses copper-mediated oxidation under these conditions, but they do not by themselves demonstrate a general anti-oxidant effect in cells, and the cellular data are therefore interpreted in terms of context-dependent cytotoxicity rather than oxidative-stress modulation. The radiolabelling studies were intended to establish proof-of-principle compatibility of the Salpyran scaffold with ^{64}Cu for potential PET imaging applications. While successful incorporation was observed, the newly identified Fe(III) preference of the ligand presents a challenge for quantitative radiolabelling. Rather than representing a failure, this finding provides critical design criteria, namely, the need to suppress Fe(III) affinity, for the future development of Salpyran-inspired frameworks tailored for radiochemical applications.

The broader cytotoxicity screen revealed that Cu-Salpyran exhibits greater intrinsic antiproliferative activity than the free ligand across several cancer cell lines. In contrast, the opposite trend was observed in carboplatin-resistant NSCLC models, where Salpyran displayed enhanced potency relative to its copper complex. These observations suggest that the biological response to the Salpyran framework is strongly dependent on cellular context. Whereas copper coordination enhances baseline cytotoxicity in multiple tumour types, the free ligand may interact differently with pathways associated with platinum resistance. While the molecular basis of these effects remains unclear, the results demonstrate that metal coordination can profoundly influence the biological behaviour of the Salpyran scaffold and provide additional motivation for the future design of structurally related systems.

It is instructive to compare Cu-Salpyran with recent copper-based therapeutic systems that operate through redox-driven cell death. The pyrazolopyrimidine Cu(II) complexes and the tripodal Cu(II) complexes both rely on intracellular copper redox chemistry, Fenton-like hydroxyl radical generation, GSH depletion, and/or cuproptotic proteotoxic stress, to achieve low-micromolar to nanomolar cytotoxicity.[33,35] Xu *et al.* similarly exploit a Cu(I) centre that is intrinsically more efficient than Cu(II) in Fenton chemistry, and they explicitly note that the precise mechanism remains unresolved.[34] Cu-Salpyran sits at the opposite end of this spectrum: EPR and UV-Vis measurements show that at pH 7.4 roughly 85% of the copper remains Cu(II) after 1 h with ascorbic acid, ascorbate consumption is minimal, and R6G degradation is suppressed even in the presence of H_2O_2 and of the reactive Cu(II)-Prs3 peptide. The complex is therefore not a pro-oxidant compared to recent examples;[33–35] and its modest, strongly cell-line-dependent cytotoxicity is unlikely to be driven primarily by ROS. This comparison refines the structure–function argument of the present work; Cu-Salpyran displays a contrasting redox profile to recently reported pro-oxidant copper-based therapeutics, suppressing copper-mediated oxidative chemistry, particularly at pH 7.4. Its N_3O coordination environment may contribute by modulating copper speciation and accessibility to reduction. However, the precise mechanism remains unresolved, and its modest, cell-line-dependent cytotoxicity suggests that its biological activity cannot be attributed solely to ROS generation. The trade-off is lower potency, but also a different and potentially complementary mechanism of action,

and a much clearer mechanistic picture than systems in which copper speciation and redox state are unresolved.

Conclusions

This study establishes Salpyran as a versatile platform for copper bioinorganic chemistry and systematically defines the structure–function boundaries of the Salpyran ligand family under aqueous conditions. Methoxy and fluoro substitution produced only modest changes in protonation and metal-binding properties and do not improve Cu(II)/Zn(II) selectivity. Direct comparison with trientine reveals revealed a pronounced preference for Fe(III), identifying an important limitation of the scaffold for selective copper chelation. Direct comparison with trientine revealed a pronounced preference for Fe(III) over Cu(II) (ΔpM $\approx$ 1.95 at pH 7.4), which is identified as a key limitation of the scaffold for Cu-selective applications and traced to the hard N_3O donor set; softening the donor atoms, enforcing steric rigidification, or modulating the phenolate pK_a while preserving aqueous solubility are proposed as design criteria for the next generation of Salpyran-derived ligands. Cu(II)-Salpyran suppresses copper-mediated ROS formation in chemical assays, limits copper-driven peptide oxidation, and binds DNA non-oxidatively. Proof-of-concept ^{64}Cu radiolabelling confirms PET compatibility, though Fe(III) competition requires framework refinement. Cytotoxicity studies reveal context-dependent activity: copper coordination enhances potency in most cancer lines but reduces it in carboplatin-resistant NSCLC models, without cross-resistance. Collectively, these findings position Cu-Salpyran relative to current pro-oxidant copper therapeutics: whereas recent Cu(II) and Cu(I) systems achieve cytotoxicity through Fenton-like ROS generation, GSH depletion, and cuproptosis.[33–35] Cu-Salpyran suppresses copper-mediated redox chemistry at physiological pH while retaining context-dependent antiproliferative activity. Redox control, rather than redox cycling, therefore, emerges as a viable design axis for copper-based anticancer agents, with metal selectivity (particularly Fe(III) *vs.* Cu(II)) and cellular context remaining the principal unresolved variables. These conclusions are experimentally grounded in the potentiometric, EPR, UV-Vis, and cytotoxicity data presented here.

Author contributions

GEK devised the project with critical input from RP, CK and MKL. AE, AD, SW, JD, and NBE synthesised and characterised Salpyran and its derivatives with input from JS, while SW performed oxidation studies. AG, NB and CK performed solution and oxidation studies. MKL performed EPR, DNA and oxidation studies. GF performed radiolabelling studies. NS, LC, EJM, KO, JB, MW, MM, JC, performed cancer cell studies at Sussex. PL, IO performed cancer cell studies in Germany. GEK wrote the paper with critical inputs from AE, RP, CK, MKL, IO, LC and EJM. All authors read and approved the final manuscript.

Conflicts of interest

There are no conflicts to declare.

Data availability

All data generated or analyzed during this study are included in this published article and its supplementary information (SI). SI contains experimental procedures, synthetic and spectroscopic characterisation data (NMR and HRMS), protonation and metal-complex stability constants, potentiometric speciation diagrams, EPR and UV–Vis measurements, DNA interaction studies, ^{64}Cu radiolabelling protocols, and supplementary cytotoxicity data. Supplementary information is available. See DOI: https://doi.org/10.1039/d6dt02297a.

Acknowledgements

AE thanks the Kroto JRA award (summer 2023) for a summer research placement. GEK thanks the Ewart Bequest for funding for a summer placement (JD, summer 2021). NBE thanks TETfUND for a PhD scholarship.

References

1 J. A. Drewry and P. T. Gunning, *Coord. Chem. Rev.*, 2011, **255**, 459–472.
2 R. Tabti, N. Tounsi, C. Gaiddon, E. Bentouhami and L. Desaubry, *Med. Chem.*, 2017, **07**, 875–879.
3 C. Santini, M. Pellei, V. Gandin, M. Porchia, F. Tisato and C. Marzano, *Chem. Rev.*, 2014, **114**, 815–862.
4 C. Marzano, M. Pellei, F. Tisato and C. Santini, *Adv. Anticancer Agents Med. Chem.*, 2012, **9**, 185–211.
5 Y. Wang, T. Tang, Y. Yuan, N. Li, X. Wang and J. Guan, *ChemMedChem*, 2024, **19**, e202400060.
6 J. R. J. Sorenson, in *Biology of Copper Complexes*, Humana Press, 1987, pp. 3–16.
7 C. Duncan and A. R. White, *Metallomics*, 2012, **4**, 127–138.
8 M. Wehbe, A. W. Y. Leung, M. J. Abrams, C. Orvig and M. B. Bally, *Dalton Trans.*, 2017, **46**, 10758–10773.
9 O. Krasnovskaya, A. Naumov, D. Guk, P. Gorelkin, A. Erofeev, E. Beloglazkina and A. Majouga, *Int. J. Mol. Sci.*, 2020, **21**, 3965.
10 J. Ashraf and M. A. Riaz, *Turk. J. Chem.*, 2022, **46**, 595–623.
11 L. M. Balsa, L. Santa, M. d. la Parra, O. Espindola-Moreno and I. E. León, *Drug Discovery Today*, 2025, **30**, 104522.
12 S. S. Hindo, M. Frezza, D. Tomco, M. J. Heeg, L. Hryhorczuk, B. R. McGarvey, Q. P. Dou and C. N. Verani, *Eur. J. Med. Chem.*, 2009, **44**, 4353–4361.
13 C. Duncan and A. R. White, *Metallomics*, 2012, **4**, 127–138.
14 G. G. Rocha, L. M. S. Ramos, L. A. S. Barbosa, R. P. Siqueira, F. C. da Silva, D. C. Brandão, P. M. A. P. Lima, A. C. P. de Matos, A. L. Bogado, G. P. Guedes, J. A. L. C. Resende, G. d. M. Pereira,

 This journal is © The Royal Society of Chemistry 2026

P. P. Corbi, W. Guerra and T. G. de Araújo, *ACS Omega*, 2026, **11**, 687–699.
15 J. J. Bartnicka, F. Al-Salemee, G. Firth and P. J. Blower, *Metallomics*, 2020, **12**, 1508–1520.
16 U. Ndagi, N. Mhlongo and M. E. Soliman, *Drug Des., Dev. Ther.*, 2017, **11**, 599–616.
17 C. Molinaro, A. Martoriati, L. Pelinski and K. Cailliau, *Cancers*, 2020, **12**, 1–26.
18 Q. Peña, S. Rodríguez-Calado, A. J. Simaan, M. Capdevila, P. Bayón, O. Palacios, J. Lorenzo and O. Iranzo, *Front. Pharmacol.*, 2022, **13**, 1060827.
19 M. M. Le Roy, S. Héry, N. Saffon-Merceron, C. Platas-Iglesias, T. Troadec and R. Tripier, *Inorg. Chem.*, 2023, **62**, 8112–8122.
20 S. Dasari and P. B. Tchounwou, *Eur. J. Pharmacol.*, 2014, **740**, 364–378.
21 A. Mariconda, J. Ceramella, A. Catalano, C. Saturnino, M. S. Sinicropi and P. Longo, *Inorganics*, 2025, **13**, 246.
22 C. E. Elwell, N. L. Gagnon, B. D. Neisen, D. Dhar, A. D. Spaeth, G. M. Yee and W. B. Tolman, *Chem. Rev.*, 2017, **117**, 2059–2107.
23 M. Murali, A. K. Mala, S. Sangeetha, B. Selvakumaran, P. A. Prakash, S. Shanmugavadivel, T. A. Kamal and M. S. M. Jaabir, *Dalton Trans.*, 2026, **55**, 5466–5484.
24 S. Wei, H. Zhang, Z. Fang, J. Shi, B. Li, Z. Liu, Y. Song, J. Xu, Q. Yu, M. Zhang and K. Liu, *Results Eng.*, 2026, **29**, 109429.
25 M. Nguyen, L. Vendier, J.-L. Stigliani, B. Meunier and A. Robert, *Eur. J. Inorg. Chem.*, 2017, **2017**, 600–608.
26 W. Zhang, D. Huang, M. Huang, J. Huang, D. Wang, X. Liu, M. Nguyen, L. Vendier, S. Mazères, A. Robert, Y. Liu and B. Meunier, *ChemMedChem*, 2018, **13**, 684–704.
27 Y. Li, M. Nguyen, M. Baudoin, L. Vendier, Y. Liu, A. Robert and B. Meunier, *Eur. J. Inorg. Chem.*, 2019, **2019**, 4712–4718.
28 A. Lakatos, É. Zsigó, D. Hollender, N. V. Nagy, L. Fülöp, D. Simon, Z. Bozsó and T. Kiss, *Dalton Trans.*, 2010, **39**, 1302–1315.
29 L. Lannfelt, K. Blennow, H. Zetterberg, S. Batsman, D. Ames, J. Harrison, C. L. Masters, S. Targum, A. I. Bush, R. Murdoch, J. Wilson and C. W. Ritchie, *Lancet Neurol.*, 2008, **7**, 779–786.
30 T. Storr, M. Merkel, G. X. Song-Zhao, L. E. Scott, D. E. Green, M. L. Bowen, K. H. Thompson, B. O. Patrick, H. J. Schugar and C. Orvig, *J. Am. Chem. Soc.*, 2007, **129**, 7453–7463.
31 S. Noël, S. B. Rodriguez, S. Sayen, E. Guillon, P. Faller and C. Hureau, *Metallomics*, 2014, **6**, 1220–1222.
32 S. Noël, F. Perez, J. T. Pedersen, B. Alies, S. Ladeira, S. Sayen, E. Guillon, E. Gras and C. Hureau, *J. Inorg. Biochem.*, 2012, **117**, 322–325.
33 K. Yang, Q. Chen, J. Chen, L. F. Geng, M. X. Ma, Y. Q. Gu, M. I. Choudhary, H. Liang and Z. F. Chen, *J. Med. Chem.*, 2025, **68**, 7137–7152.
34 S. Xu, Y. Hao, X. Xu, L. Huang, Y. Liang, J. Liao, J. R. Yang, Y. Zhou, M. Huang, K. Z. Du, C. Zhang and P. Xu, *J. Med. Chem.*, 2024, **67**, 7911–7920.
35 R. Zimmermann, N. Montesdeoca and J. Karges, *J. Med. Chem.*, 2025, **68**, 12258–12271.
36 M. Strianese, D. Guarnieri, M. Lamberti, A. Landi, A. Peluso and C. Pellecchia, *Inorg. Chem.*, 2020, **59**, 15977–15986.
37 Y. Tong, B. Liu, Y. Wu, B. Yang, G. Wen, Y. T. Yang, J. Chai and X. Hu, *Sens. Actuators, B*, 2017, **252**, 794–802.
38 P. Yadav, O. Blacque, A. Roodt and F. Zelder, *Inorg. Chem. Front.*, 2021, **8**, 4313–4323.
39 E. Y. L. Hui, D. W. P. Tay, J. A. Richard, Z. Pohancenikova, K. Renault, A. Romieu and Y. H. Lim, *Dyes Pigm.*, 2022, **207**, 110708.
40 B. Das, M. Dolai, A. Dhara, S. Mabhai, A. Jana, S. Dey and A. Misra, *Anal. Sci. Adv.*, 2021, **2**, 447–463.
41 P. Ju, Q. Su, Z. Liu, X. Li, B. Guo, W. Liu, G. Li and Q. Wu, *J. Mater. Sci.*, 2019, **54**, 851–861.
42 A. Jayaraj, M. S. Gayathri, G. Sivaraman and C. A. S. P, *J. Photochem. Photobiol., B*, 2022, **226**, 112371.
43 T. Zhu, Q. Gou, Y. Yang, Y. Zhang and M. Chen, *J. Mol. Struct.*, 2022, **1264**, 133258.
44 J. C. Pessoa and I. Correia, *Coord. Chem. Rev.*, 2019, **388**, 227–247.
45 R. Purchase, *Sci. Prog.*, 2013, **96**, 19–32.
46 S. H. Laurie and B. Sarkar, *J. Chem. Soc., Dalton Trans.*, 1977, 1822–1827.
47 J. I. Lachowicz, A. H. Emwas, G. R. Delpiano, A. Salis, M. Piludu, L. Jaremko and M. Jaremko, *Adv. Mater. Interfaces*, 2020, **7**, 2000544.
48 V. M. Nurchi, G. Crisponi, M. Crespo-Alonso, J. I. Lachowicz, Z. Szewczuk and G. J. S. Cooper, *Dalton Trans.*, 2013, **42**, 6161–6170.
49 A. Ala, E. Aliu and M. L. Schilsky, *Dig. Dis Sci.*, 2015, **60**, 1433–1439.
50 F. T. Kirk, D. E. Munk, E. S. Swenson, A. M. Quicquaro, M. H. Vendelbo, M. L. Schilsky, P. Ott and T. D. Sandahl, *Hepatology*, 2024, **79**, 1065–1074.
51 B. C. Dickinson and C. J. Chang, *Nat. Chem. Biol.*, 2011, **7**, 504–511.
52 A. E. Behar, L. Sabater, M. Baskin, C. Hureau and G. Maayan, *Angew. Chem., Int. Ed.*, 2021, **60**, 24588–24597.
53 J. Devonport, N. Bodnár, A. McGown, M. B. Maina, L. C. Serpell, C. Kállay, J. Spencer and G. E. Kostakis, *Inorg. Chem.*, 2021, **60**, 15310–15320.
54 G. E. Kostakis, *Dalton Trans.*, 2023, **52**, 18118–18132.
55 A. Idrissi, B. Marekha, M. Barj and P. Jedlovszky, *J. Phys. Chem. B*, 2014, **118**, 8724–8733.
56 T. Magsumov, A. Fatkhutdinova, T. Mukhametzyanov and I. Sedov, *Biomolecules*, 2019, **9**, 547.
57 S. Wernersson, S. Birgersson and M. Akke, *Biochemistry*, 2023, **62**, 44–52.
58 N. Mohan, C. V. Vidhya, V. Suni, J. M. Ameer, N. Kasoju, P. V. Mohanan, S. S. Sreejith and M. R. P. Kurup, *New J. Chem.*, 2022, **46**, 12540–12550.
59 N. Mohan, S. S. Sreejith, M. E and M. R. P. Kurup, *J. Mol. Struct.*, 2026, **1355**, 144968.

60 E. P. Gillis, K. J. Eastman, M. D. Hill, D. J. Donnelly and N. A. Meanwell, *J. Med. Chem.*, 2015, **58**, 8315–8359.
61 S. Purser, P. R. Moore, S. Swallow and V. Gouverneur, *Chem. Soc. Rev.*, 2008, **37**, 320–330.
62 I. Ojima, *Fluorine in Medicinal Chemistry and Chemical Biology*, Wiley-Blackwell, Chichester, 2009, pp. 1–624.
63 W. K. Hagmann, *J. Med. Chem.*, 2008, **51**, 4359–4369.
64 J. Peisach and W. E. Blumberg, *Arch. Biochem. Biophys.*, 1974, **165**, 691–708.
65 G. Csire, L. Nagy, K. Várnagy and C. Kállay, *J. Inorg. Biochem.*, 2017, **170**, 195–201.
66 M. Sharifi-Rad, N. V. A. Kumar, P. Zucca, E. M. Varoni, L. Dini, E. Panzarini, J. Rajkovic, P. V. T. Fokou, E. Azzini, I. Peluso, A. P. Mishra, M. Nigam, Y. El Rayess, M. El Beyrouthy, L. Polito, M. Iriti, N. Martins, M. Martorell, A. O. Docea, W. N. Setzer, D. Calina, W. C. Cho and J. Sharifi-Rad, *Front. Physiol.*, 2020, **11**, 552535.
67 C. Cheignon, P. Faller, D. Testemale, C. Hureau and F. Collin, *Metallomics*, 2016, **8**, 1081–1089.
68 M. K. Lesiów, M. Witwicki, N. K. Tan, M. E. Graziotto and E. J. New, *Chem. – Eur. J.*, 2023, **29**, e202301530.
69 J. Grau, R. F. Brissos, J. Salinas-Uber, A. B. Caballero, A. Caubet, O. Roubeau, L. Korrodi-Gregório, R. Pérez-Tomás and P. Gamez, *Dalton Trans.*, 2015, **44**, 16061–16072.
70 M. Okafor, P. Gonzalez, P. Ronot, I. El Masoudi, A. Boos, S. Ory, S. Chasserot-Golaz, S. Gasman, L. Raibaut, C. Hureau, N. Vitale and P. Faller, *Chem. Sci.*, 2022, **13**, 11829–11840.
71 S. Krishnaswamy, V. Ragupathi, S. Raman, P. Panigrahi and G. S. Nagarajan, *Polym. Bull.*, 2019, **76**, 5213–5231.
72 M. K. Lesiów and K. Krupa, *New J. Chem.*, 2021, **45**, 8543–8556.
73 A. K. Somavarapu and K. P. Kepp, *J. Neurochem.*, 2016, **137**, 101–111.
74 M. Dükkanci, G. Gündüz, S. Yilmaz and R. V. Prihod'ko, *J. Hazard. Mater.*, 2010, **181**, 343–350.
75 Y. Liu, Y. Wang, H. Li, X. Guan, L. Zhu, M. Xue, Y. Yan, V. Valtchev, S. Qiu and Q. Fang, *Chem. Sci.*, 2019, **10**, 10815–10820.
76 G. Firth, J. E. Blower, J. J. Bartnicka, A. Mishra, A. M. Michaels, A. Rigby, A. Darwesh, F. Al-Salemee and P. J. Blower, *RSC Chem. Biol.*, 2022, **3**, 495–518.
77 F. T. Kirk, D. E. Munk, E. S. Swenson, A. M. Quicquaro, M. H. Vendelbo, M. L. Schilsky, P. Ott and T. D. Sandahl, *Hepatology*, 2024, **79**, 1065–1074.
78 T. D. Sandahl, L. C. Gormsen, K. Kjærgaard, M. H. Vendelbo, D. E. Munk, O. L. Munk, D. Bender, S. Keiding, K. H. Vase, K. Frisch, H. Vilstrup and P. Ott, *Hepatology*, 2022, **75**, 1461–1470.
79 A. Piccardo, F. Paparo, M. Puntoni, S. Righi, G. Bottoni, L. Bacigalupo, S. Zanardi, A. DeCensi, G. Ferrarazzo, M. Gambaro, F. G. Ruggieri, F. Campodonico, L. Tomasello, L. Timossi, S. Sola, E. Lopci and M. Cabria, *J. Nucl. Med.*, 2018, **59**, 444–451.
80 J. J. Bartnicka, F. Al-Salemee, G. Firth and P. J. Blower, *Metallomics*, 2020, **12**, 1508–1520.
81 E. M. Andreozzi, J. B. Torres, K. Sunassee, J. Dunn, S. Walker-Samuel, I. Szanda and P. J. Blower, *Metallomics*, 2017, **9**, 1622–1633.
82 H. Sung, J. Ferlay, R. L. Siegel, M. Laversanne, I. Soerjomataram, A. Jemal and F. Bray, *CA Cancer J. Clin.*, 2021, **71**, 209–249.
83 N. Shahabadi, S. Kashanian and F. Darabi, *Eur. J. Med. Chem.*, 2010, **45**, 4239–4245.
84 Q. Peña, J. Lorenzo, G. Sciortino, S. Rodríguez-Calado, J. D. Maréchal, P. Bayón, A. J. Simaan, O. Iranzo, M. Capdevila and Ò. Palacios, *J. Inorg. Biochem.*, 2019, **195**, 51–60.
85 A. Ozdemir, O. F. Sarioglu and T. Tekinay, *Biol. Trace Elem. Res.*, 2015, **168**, 508–515.
86 S. K. Chandraker, M. Lal, P. Dhruve, R. P. Singh and R. Shukla, *Front. Mol. Biosci.*, 2021, **7**, 593040.
87 N. Shahabadi, S. Kashanian, M. Khosravi and M. Mahdavi, *Transition Met. Chem.*, 2010, **35**, 699–705.
88 R. P. Paitandi, V. Sharma, V. D. Singh, B. K. Dwivedi, S. M. Mobin and D. S. Pandey, *Dalton Trans.*, 2018, **47**, 17500–17514.
89 E. Robles-Escajeda, A. Martínez, A. Varela-Ramirez, R. A. Sánchez-Delgado and R. J. Aguilera, *Cell Biol. Toxicol.*, 2013, **29**, 431–443.
90 C. J. Kimbrough and T. R. Cundari, *ACS Omega*, 2025, **10**, 42006–42018.
91 T. Miao, Q. Deng, H. Gao, X. Fu and S. Li, *J. Chem. Inf. Model.*, 2018, **58**, 859–866.
92 J. Hormann, O. Verbitsky, X. Zhou, B. Battistella, M. van der Meer, B. Sarkar, C. Zhao and N. Kulak, *Dalton Trans.*, 2023, **52**, 3176–3187.
93 J. Borrás, G. Alzuet, M. González-Alvarez, J. L. García-Giménez, B. Macías and M. Liu-González, *Eur. J. Inorg. Chem.*, 2007, **2007**, 822–834.

 This journal is © The Royal Society of Chemistry 2026